AFGL-TR-88-0006

GRAVITY GRADIOMETER SURVEY SYSTEM (GGSS) POST-MISSION DATA PROCESSING

Dr. Sam C. Bose

APPLIED SCIENCE ANALYTICS, INC.
7049 Owensmouth Avenue
Canoga Park, CA 91303

August 1987

Final Report
May 1984 – May 1987

Prepared for:
AIR FORCE GEOPHYSICS LABORATORY
AIR FORCE SYSTEMS COMMAND
United States Air Force
Hanscom AFB, Massachusetts 01731

This technical report has been reviewed and is approved for publication.

[redacted], Capt USAF
Contract Manager

[redacted], Chief
Geodesy & Gravity Branch

FOR THE COMMANDER

[redacted], Acting Director
Earth Sciences Division

This report has been reviewed by the ESD Public Affairs Office (PA) and is releasable to the National Technical Information Service (NTIS).

Qualified requestors may obtain additional copies from the Defense Technical Information Center. All others should apply to the National Technical Information Service.

If your address has changed, or if you wish to be removed from the mailing list, or if the addressee is no longer employed by your organization, please notify AFGL/DAA, Hanscom AFB, MA 01731-5000. This will assist us in maintaining a current mailing list.

Do not return copies of this report unless contractual obligations or notices on a specific document requires that it be returned.

REPORT DOCUMENTATION PAGE

1a REPORT SECURITY CLASSIFICATION Unclassified	1b. RESTRICTIVE MARKINGS
2a. SECURITY CLASSIFICATION AUTHORITY	3. DISTRIBUTION / AVAILABILITY OF REPORT Approved for public release; Distribution unlimited
2b. DECLASSIFICATION / DOWNGRADING SCHEDULE	
4. PERFORMING ORGANIZATION REPORT NUMBER(S)	5. MONITORING ORGANIZATION REPORT NUMBER(S) AFGL-TR-88-0008
6a NAME OF PERFORMING ORGANIZATION Applied Science Analytics, Inc 6b OFFICE SYMBOL (If applicable)	7a. NAME OF MONITORING ORGANIZATION Air Force Geophysics Laboratory
6c. ADDRESS (City, State, and ZIP Code) 7049 Owensmouth Avenue Canoga Park, CA 91303	7b ADDRESS (City, State, and ZIP Code) Hanscom AFB Massachusetts 01731-5000
8a. NAME OF FUNDING / SPONSORING ORGANIZATION 8b OFFICE SYMBOL (If applicable)	9 PROCUREMENT INSTRUMENT IDENTIFICATION NUMBER F19628-84-C-0108
8c. ADDRESS (City, State, and ZIP Code)	10 SOURCE OF FUNDING NUMBERS

PROGRAM ELEMENT NO	PROJECT NO	TASK NO	WORK UNIT ACCESSION NO
63701B	3204	DM	AG

11 TITLE (Include Security Classification)
Gravity Gradiometer Survey System (GGSS) Post-Mission Data Processing

12 PERSONAL AUTHOR(S)
Sam C. Bose

13a TYPE OF REPORT	13b. TIME COVERED	14. DATE OF REPORT (Year, Month, Day)	15 PAGE COUNT
FINAL REPORT	FROM May 84 TO May 87	1987 August	76

16 SUPPLEMENTARY NOTATION

17 COSATI CODES			18 SUBJECT TERMS (Continue on reverse if necessary and identify by block number)
FIELD	GROUP	SUB-GROUP	Gravity gradiometry, Post-mission processing, Mass distribution layers, Laplace's equation, Non-stationary non-isotropic covariance, Karhunen-Loeve, Toeplitz matrix, Cosine transforms

19 ABSTRACT (Continue on reverse if necessary and identify by block number)

Post-mission processing of local airborne gravity gradient measurements simultaneously in a computationally efficient manner is addressed. The gravity signal model is obtained by solving Laplace's equation with the unknown mass distribution below the surface of the earth modelled as one or more two-dimensional(2D) white noise layers representing the vertical derivative of the disturbance potential to any order. A non-stationary non-isotropic disturbance potential covariance is obtained by invoking the Karhunen-Loeve condition on the unkown coefficients of the series solution. 2D grids of the six gravity gradients contaminated by additive white noise is the measurement model. For gaussian noise statistics closed form solutions of the continuous domain optimal estimator for each Karhunen-Loeve coefficient is obtained as a linear functional of all the measurement data. Utilization of toeplitz circulant properties of sine and cosine transforms permits discretization of the continuous algorithm as a sequence of matrix multiplications without any necessity of matrix inversions. From the Karhunen-Loeve coefficient estimates, 2D grid estimates of the gravity vector components at any altitude and at any grid spacing are obtained by performing appropriate left and right sine and cosine transforms.

20. DISTRIBUTION / AVAILABILITY OF ABSTRACT	21. ABSTRACT SECURITY CLASSIFICATION
☐ UNCLASSIFIED/UNLIMITED ☒ SAME AS RPT. ☐ DTIC USERS	Unclassified
22a NAME OF RESPONSIBLE INDIVIDUAL Vishnu V. Nevrekar, Capt, USAF	22b. TELEPHONE (Include Area Code) / 22c OFFICE SYMBOL AFGL/LWH

Contents

List of Figures

1 INTRODUCTION

1.1 Background Review

Airborne measurements of gravity were initiated back in the late fifties when the concept of airborne gravimetry was first tested by *Thompson* (1959). Although the possibility of success seemed rather remote at that time considerable work continued in airborne gravimetry by *Nettleton et. al.* (1960), *Coons et. al.* (1962), *Gumert* and *Cobb* (1970), *Szabo* and *Anthony* (1971), *La Coste et. al.* (1977). Only recently, however, airborne gravity surveys have met with considerable success as reported by *Hammer* (1982, 1983) and *Brozena* (1984). The major advantages of airborne gravimetry include speed, efficiency, uniformity of data quality and coverage over otherwise inaccessible areas. The major problem with airborne gravimetry, however, is the inability to separate gravitational forces from inertial forces (*Meissl*, 1970).

The problem of separating inertial and gravitational forces motivated the development of airborne gravity gradiometry where the inertial and gravitational forces are separated by mounting three gravity gradiometer sensors on an inertially stabilized platform (*Moritz*, 1967, 1971). A gravity gradiometer measures the six second order gravity gradients. By eliminating the effect of the earth's normal gravity field from these six gravity gradients, one obtains the gravity gradients of the anomalous potential. These second-order gravity gradients provide short-wavelength (high frequency) information particularly suitable for a precise determination of the anomalous gravity field in a local area. In addition, the high frequencies of the anomalous gravity field provide useful information for geophysical prospecting (*Jordan*, 1978; *Brown*, 1981).

Hardware development for the gravity gradiometers began towards the end of the sixties and has continued since then. During the seventies four gravity gradiometers were under development: the Rotating Gravity Gradiometer of Hughes Research Laboratories (*Forward*, 1971), the Spherical Floated Gravity Gradiometer of Charles Stark Draper Laboratory (*Trageser*, 1970, 1975), the Rotating Accelerometer Gravity Gradiometer of Bell Aerospace/Textron (*Metzger* and *Jircitano*, 1977, 1981) and the Superconducting Gravity Gradiometer of the University of Maryland (*Paik*, 1976, 1981, 1985). Of these four, only two are currently under development, the Bell Rotating Accelerometer Gravity Gradiometer system now known as the Gravity Gradiometer Survey System (GGSS) and the Superconducting Gravity Gradiometer developed by Paik and his coworkers at the University of Maryland. The Superconducting Gravity Gradiometer is planned to be used for satellite gradiometry. (*Paik et. al.*, 1978) The GGSS is the one which will be employed for airborne gradiometery.

1.2 Purpose and Scope

The purpose of this research is to develop a methodology for processing GGSS survey data. The GGSS consists of three gravity gradiometer instruments (GGI's) mounted in an

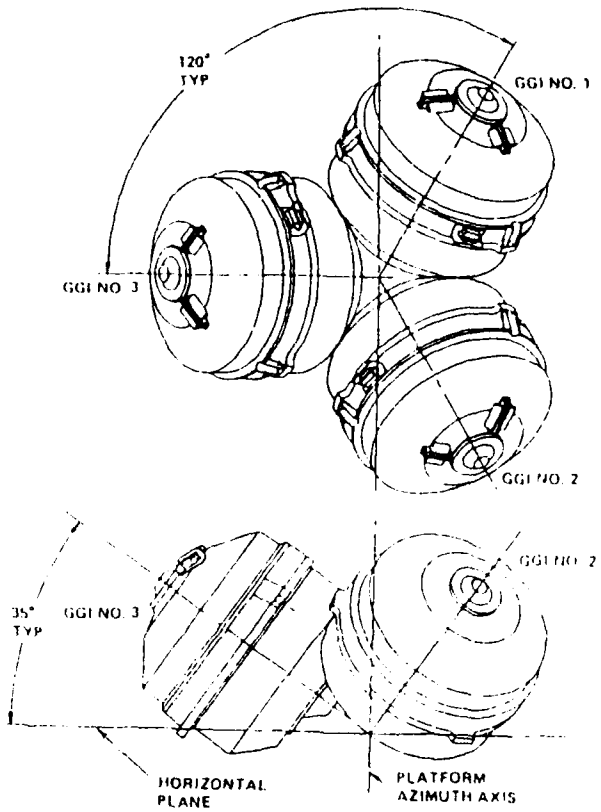

Figure 1: GGI Orientation

'umbrella' configuration of 35 degrees as shown in Figure 1 aboard a stabilized platform together with the associated electronics, GPS receiver, and a Rolm computer. The platform contains gyros and accelerometers and operates as a navigator using GPS position updates, thus establishing a coordinate frame for gradiometer measurements. To define the complete gravity gradient field requires three GGI's. The umbrella configuration was chosen so that each GGI will be in the same inertial environment. A total of six gradient measurements are made in the orthogonal system of the umbrella angle, which is sufficient to define the total gravity field.

Gravity gradients are sensed by differencing the accelerations measured by two high precision Bell Aerospace accelerometers. Two pairs of accelerometers are mounted along the edge of a nine inch disk, with their sensitive axes tangent. Outputs of opposite pairs, with sensitive axes 180 degrees out of phase, are summed, and the outputs of the pairs are differenced. With this arrangement, any linear accelerations to the disk will not be registered by the combined output. However, if an acceleration field exists with the specific force higher on one side of the disk than the other , an unbalance will result and the slope of the acceleration field will be the output.

In the Bell Aerospace GGI's, the disk is slowly rotated. When rotation occurs, the combined output becomes sinusoidal with the amplitude proportional to the magnitude of the gradient and the frequency equal to two times the rotation rate. This procedure has the effect of shifting the frequency of the gradient signal from DC to twice the wheel rate. It now becomes possible to bandpass filter the gradient outputs, eliminating much of the noise. When the signal is demodulated, we get inline and cross gradients. Thus, the outputs of the GGSS, recorded on the data tape, are six gravity gradient elements in the umbrella angle reference frame.

The data processing falls naturally into two stages. The first stage is temporal wherein the data processing demodulates the survey system output, compensates the output for the effects of pressure, temperature, drift rate and self gradients and low pass filters the data to produce a data tape with one second samples of the gradients. Gradients are still in the instrument coordinate system, the umbrella angle. The second stage is spatial and, therefore, two dimensional in nature and consists of gridding, terrain correction, interpolation, smoothing, integration, downward continuation, and incorporation of astrogeodetic tie points. The compensated, demodulated, and filtered gradient signal after Stage I processing will be lined up with time synchronized position data from the aircraft on-board computer and sampled spatially at 1 Km intervals corresponding to the survey grid. Ideally, the 1 Km data obtained from the Stage I processing will coincide with the survey grid. However, due to navigation and aircraft control errors, the actual tracks flown will deviate from the ideal survey tracks by up to a few tenths of a kilometer. The initial operation in Stage II processing will be a data gridding exercise where an interpolation algorithm (a local least squares collocator) will be used to line up the actual gradient data with the survey grid.

Stage I data processing as well as the initial data gridding of Stage II are not within

the scope of this effort and henceforth not discussed in this report any further. Hence, it is assumed that Stage I processing and Stage II data gridding have been successfully performed with the end product being regular two-dimensional grids of gravity gradient measurements of the anomalous potential. Furthermore, it is assumed that the altitude of the survey airplane is constant within small bounds.

1.3 Problem Statement

The objective of this research effort was to devise a methodology to process two-dimensional grids of gravity gradients at survey altitude to yield gravity disturbance vector estimates at the surface of the earth.

1.4 Research Objective

The measured gravity gradients are the six elements of the gradient tensor. An actual airborne gradiometer survey over an area 300×300 Km consisting of bidirectional flight paths 5 Km apart with along-track sampling intervals of 1 Km will result in approximately 220,000 measurements. The main problem with the determination of the gravity field from airborne gradiometery is the huge amount of gradient data collected during a gradiometry survey. The primary objective of this research effort was to solve the problem of processing all the airborne gravity gradient measurements simultaneously in a computationally efficient manner without neglecting gradiometer measurement noise.

1.5 Survey of Techniques

GGSS data processing methods proposed to date are primarily based on least squares collocation, an excellent review of which is presented in *Moritz* (1980). The method of least squares collocation was employed by *Schwarz* (1977) for the computation of the vertical gravity disturbance vector from simulated gravity gradient data. Due to the limited extent of the survey data a low frequency part had been subtracted which resulted in the estimation of the residual gravity field. His simulation results showed that $15' \times 15'$ mean disturbance could be estimated to an accuracy of 2.2 mgals with a profile spacing of $20'$. In the same study it was found that the estimates wil. get worse if the gradient data are corrupted by systematic errors.

Least squares collocation involves the inversion of a matrix of order equal to the number of measurements. Since the number of measurements collected during the airborne GGSS test is expected to be approximately 2×10^5, a full scale least squares collocation approach is presently impractical. A template method (*Goldstein* and *White*, 1985) exploits the attenuation with distance in the correlations between gravity gradients. By averaging the measurements over compartments whose sizes increase with distance from the estimation point the number and density of observations are reduced significantly. Thus, the short

wavelengths of gradients in distant zones which signify local density contrasts and have minimal correlation with the estimate are averaged out, while the longer wavelengths are retained. The averaging compartments form a template centered directly above the estimation point, hence the name 'template method'. Once the data set with large numbers of points has been transformed to a much smaller set of averages the gravity disturbance vector is estimated using space domain least squares collocation. This method requires generation of covariances between gravity gradient averages implying the necessity of a covariance model that is amenable to analytic integration. The covariance function used for the template method is the Attenuated White Noise (AWN) model (*Heller* and *Jordan*, 1979). The template method is simplest for uniformly spaced data, since a fixed template design can be utilized. However, for non uniformly spaced data the template needs to be restructured and the weights for each template zone recomputed again for each estimation point. To redefine the zones and recompute the optimal weights a matrix of order equal to the number of template zones needs to be inverted.

Another space-domain method for processing GGSS data is based on *Rummel's* (1982) technique of developing an integral formula estimator that is optimized for the effect of measurement noise. This method was developed as an alternative to the inverse Stokes integral for processing large, densely spaced satellite altimetry data without ignoring measurement errors. Assuming flat earth approximation *Jekeli* (1984) extended the idea to incorporate heterogeneous gravity gradient data sets at altitude. The appropriate Kernel function is expressed as a Fourier transform of its spectrum which in the flat earth approximation is fitted by pieces of powers of spatial frequency and thereby amenable to analytical integration. Thus, from each set of measured gradients the whole gravity disturbance vector can be recovered. Gravity disturbance vector estimates from different sets of gravity gradient measurements can be combined in a least squares adjustment to provide the final estimate (*Jekeli*, 1984). A further enhancement to the estimator was proposed by *Jekeli* (1985) wherein a method to integrate isolated surface tie-point data was described. However, the estimator assumes infinitely extended gradient data and does not assign sufficient weight to the tie-point data. Thus, there is no reproducibility at the tie-point data as with optimal least-squares collocation. Hence, the incorporation of tie-point data is not optimal in this estimator. On the other hand, without incorporating tie-points *Jekeli's* (1985) simulation results show that a noticeable bias and trend could not be estimated from the given gradient data. Also, because of the lack of data outside the survey area, estimates near the edge are distorted and unreliable. One limitation of this method is the requirement that the data be on a plane of constant altitude. Furthermore, to recover the gravity disturbance vector at the surface of the earth downward continuation has to be performed.

Another technique based on Stokes' theorem has been proposed by *Rufty* (1986) wherein the connection between cross products of vector fields and line integrals of gradients is exploited. For conservative fields, the constraint of zero cross product of the vector field is equivalent to zero closed line integrals of the gradients. This fact is exploited in this

method to recognize that due to the presence of noise these gradient line integrals are path dependent. The method computes the best estimates of segment integrals and then combines the estimates from the various paths. Thus, the algorithm simultaneously weights all possible path integrals of the gradient to yield an optimal estimate of the disturbance. The method considers all paths simultaneously but does not include any modeling of the statistics of the field. The gravity estimates are obtained at the survey altitude from gradient track data at altitude. Thus, to recover the gravity disturbance vector at the surface of the earth downward continuation has to be performed.

A combination of least-squares collocation in the space domain and Wiener filtering in the frequency domain has been proposed by Bell Aerospace/Textron (*Hutcheson*, 1985; *Hutcheson* and *Grierson*, 1985). The least squares collocator is used to estimate the low frequency component of gravity disturbance on a sparse grid. This is then combined in the frequency domain with the complementary high frequency disturbance estimate obtained from the Wiener smoother. The resulting map is then transformed back into the space domain. For both the low and high frequency parts of the spectrum, plane integration at flying altitude and downward continuation are carried out in one step. The instrument red noise part of the measurement error is filtered by the Wiener smoother in the frequency domain. Thus, the gradient data needs to be on a two-dimensional grid. The application of this method for the estimation of the gravity disturbance vector at the surface of the earth from gradient data at survey altitude does not provide accurate results at the edges of the area due to spectral leakage.

Another method that is based completely on frequency domain approach was proposed by *Vassiliou* (1985, 1986). The method is based on the application of multiple input-single output filtering equations, using as inputs the linearly correlated second-order gravity gradients and as output the first-order gradients. In this way, each first-order gradient is estimated from a combination of its gradients in the frequency domain. The method uses all the gradient measurements at once for the whole area. To make the method computationally efficient, the Fast Fourier Transform (FFT) is employed. In this method, gradient plane integration and downward continuation are performed in one step using FFT techniques. This method, as in any frequency domain technique, suffers from spectral leakage. Additionally, it requires the data points to be on a regular two-dimensional grid and assumes flat earth approximation.

Parametric least squares estimation is the key to another method where the measured gravity gradients are represented as a set of parameters pre-multiplied by a design matrix observed in additive noise (*Peacock*, 1985; *Center* and *Peacock*, 1985). The parameters can be point masses, spherical harmonics, two-dimensional Fourier coefficients or Hankel transform coefficients. In practice, the parameters used are Fourier series coefficients. Thus, the design matrix contains sampled values of the Fourier series basis functions evaluated at the measurement points. Singular value decomposition (*Lawson* and *Hanson*, 1974) is used to decompose the design matrix into a product of a left orthogonal matrix, a middle diagonal matrix and a right orthogonal matrix. The elements of the diagonal matrix are

the singular values of the design matrix. For large sets of measurements a single singular value decomposition is computationally impractical. Therefore, a sequential singular value is applied. With this sequential singular value decomposition algorithm, measurements are processed in a sequence of relatively small batches. At each stage, previous measurement and prior probability distributions are compressed into an equivalent measurement vector. After processing the new set of measurements, the parameter space is orthogonally decomposed into three sets of linear combinations: those that are well estimated, those that are partially estimated and those that are essentially unobserved based on the magnitudes of the signal-to-noise ratios. When this sequential operation is complete, the optimal estimates of the sequential singular value decomposition states are formed and the states can be used to form optimal estimates of the disturbance vector at selected points. The application of sequential singular value decomposition makes the solution of least squares problems with large data sets computationally efficient. However, to implement a parametric least-squares algorithm, a set of basis functions must be explicitly chosen. The parameters then become the coefficients of a functional expansion in terms of these basis functions. Since the number of computations grows as the cube of the number of parameters, the choice of parameters becomes the critical design issue.

A data processing technique that transforms a gradiometer survey network into an electrical network was proposed by *Eckhardt* (1986). In this method GGSS survey data is analyzed by analyzing an electrical network that is isomorphic to the survey network. The integrated gradients between the nodes where the survey lines cross correspond to the applied voltages between the nodes of the network; the gradient variances correspond to the internodal resistances; the elements of the adjusted gravity vector correspond to the nodal voltages; and the solution variances correspond to the resistances to ground. Solving the electrical network is then equivalent to making a least squares adjustment of the survey network. The initial step is to process the raw GGSS signals to extract the elements of the gravity gradient tensor; next ground-truth measurements are upward continued to the network tie points; then the internodal adjustment is done; finally the gravity vector is calculated along the tracks between the nodes and the field is interpolated and downward continued to the reference surface. This method differs from most other techniques proposed in that it is not based on the least squares collocation and thus does not use expected correlations of the gravity field and measurements.

1.6 Technical Approach

Several different methods of GGSS data processing was discussed. Clearly the straightforward application of least squares collocation is not a practical proposition. Therefore, all the methods approach the problem with the idea of making the computations tractable. The methods are then not optimal. Some of the methods do not use any gravity field model for the survey region and those that do are restricted to homogeneous and isotropic covariances. But as *Rummel* and *Schwarz* (1977) has shown the homogeneous model may

not always be satisfactory and the structure of the anomalous potential is more realistically represented by non-homogeneous weighting functions. *Morrison* (1975, 1977) has shown that the assumption of isotropy is not always valid and *Kearsley* (May 1977, July 1977) has investigated non-stationary estimation where he shows the superiority of two-dimensional non-isotropic covariances.

Another fundamental assumption in the frequency domain techniques is the requirement of stationarity for the gravity quantities and for the measurement noise. But as *Nash* and *Jordan* (1978) pointed out, "Gravity anomalies are neither stationary nor isotropic; some areas are rough, other smooth, and most areas contain linear (non-isotropic) features corresponding to a mountain range, continental shelf, fault, etc. The non-stationary, non-isotropic character of gravity anomalies is hardly surprising since approximately 90 percent of the energy in gravity anomalies is caused by terrain (and the associated isostatic compensation at the Mohorovicic discontinuity), and most terrain contains obvious linear features." Thus the frequency domain approach, through computationally attractive really does not address the nonstationarity and nonisotropy of local gravity modeling.

Nash and *Jordan* advocate the application of random process theory to the problems of geodesy particularly in the modeling and estimation of the fine structure of the earth's gravity field. They state that: "The theoretical basis for statistical models of gravity anomalies is somewhat tenuous. 'Ensembles' and 'probability distributions' are difficult to define, since there is only one earth, and gravity at a particular point is a fixed, deterministic quantity (excluding transient effects such as tides) . . . . Nevertheless, statistical geodesy has survived (flourished!) because of the powerful conceptual, mathematical, and computational tools afforded by the statistical approach." Random process models of gravity were first used by *Hirvonen* (1956, 1962) and *Kaula* (1957, 1959) in the late 1950's. These models take the form of autocovariance functions (acf's) and spherical harmonic power spectral densities (psd's). Statistical models for the deflections were proposed by *Levine* and *Gelb* (1969) without considering the associated anomaly models. *Shaw et. al.* (1969) recognized that the Vening-Meinesz formulas provide a constraint between the anomaly and deflections; they used this constraint to derive statistical models for the deflections from theoretical anomaly models. In Particular, Shaw and his coworkers proposed the 'exponential anomaly model' and the 'Bessel anomaly model' and determined the associated deflection models. In a similar paper, *Kasper* (1971) proposed a 'second-order Markov anomaly model' and determined the associated deflection models. The models proposed by Shaw et al. and Kasper are 'self-consistent', since the anomaly and deflection statistics satisfy compatibility conditions that are based on the Vening-Meinesz equations. However these models were somewhat incomplete since even though the constraints between the anomaly and deflections were recognized, but the constraints relating to the undulation were ignored. *Jordan* (1972) took into account these constraints and proposed the 'third-order Markov undulation model' and derived 'necessary conditions' that must be satisfied in order for the anomaly, deflection, and undulation correlation functions to be physically reasonable. Other self-consistent models have also been proposed (*Tscherning*

and *Rapp*, 1974; *Tscherning*, 1976). Some of these self-consistent models are also mathematically convenient insofar as the covariance functions aloft can be expressed analytically (*Bellaire*, 1971, 1972, 1977; *Heller* and *Jordan*, 1979).

Self-consistent models are usually more complex because they involve two or more gravimetric uncertainties (vertical deflections, gravity anomaly, undulation) as opposed to ad hoc models involving only one gravimetric uncertainty. The complexity of the self-consistent models has a blessing in that it makes possible to infer a statistical model for one gravimetric uncertainty (e.g. deflections) from data pertaining to another gravimetric uncertainty (e.g. gravity anomaly). However, even in the case of self-consistent models the autocorrelation function (acf) of one of the gravimetric uncertainties is required to be hypothesized and the others derived via the constraining equations.

Some of these ad hoc or self-consistent models can be expressed in state-space form where the gravimetric uncertainties along a line (trajectory) in space can be viewed as a function of time, rather than space. By definition, a 'state-space' model is one that can be expressed as a set of linear ordinary differential equations excited by white noise. Such models are convenient and useful for covariance simulation and Kalman filtering. The 'third-order Markov undulation model' of *Jordan* (1972) is such a model. However, this is only possible because of Jordan's assumption of an isotropic acf for undulation.

As *Nash* and *Jordan* (1978) admit: "All of the above mentioned models assume stationarity and isotropy, both of which are unrealistic assumptions. One critic has said facetiously, "Statistical gravity models are nice but they disagree with the data." This criticism is embarrassingly valid. Hopefully, new models will be developed in the near future that account for nonstationarity and nonisotropy." As a result they state that the first major problem in statistical geodesy as: "Nonstationary nonisotropic models need to be developed to replace the simple models used heretofore." They further go on to advocate the application of modern estimation and control theory to geodesy acknowledging though that: "The application of modern estimation theory (Kalman filtering) to gravimetric uncertainties is complicated by the fact the the quantities of interest are two or three dimensional random processes, in the sense that two or three coordinates (e.g., north-east, north-east-down) are needed to specify them." They further state that: "The normal recursive approach ... is difficult to pursue directly for geodetic uncertainties because they are not time series, but rather they are two and three dimensional spatial random processes. For such processes it is generally not possible to write down linear differential equations ... that describe the dynamic evolution of the process. Rather it is necessary to develop partial differential equations, which when excited by two-or-three-dimensional white noise, 'produce' the desired statistics. This is a difficult theoretical problem; even if done correctly, it is not clear how to solve the estimation problem."

Motivated by these remarks the approach taken here is to exploit the marriage of physical geodesy and random process theory. We shall solve Laplace's equation with the unknown mass distribution below the surface of the earth modelled as a two-dimensional white noise layer representing the vertical derivative of the disturbance potential to any

pre-specified order. This results in a series solution of the disturbance potential wherein the unknown coefficients of the expansion are forced to be uncorrelated by invoking the Karhunen-Loève condition. It is shown that the disturbance potential covariance obtained from this model is both non-stationary and non-isotropic.

Next, the six (6) gravity gradient measurements are represented in terms of the Karhunen-Loève series expansion of the disturbance potential resulting in six basis functions. These basis functions are shown to be orthogonal. A linear mean square estimator utilizing all the gravity gradient measurements simultaneously is obtained in continuous domain by solving an integral equation involving the estimator gains which are represented by the same orthogonal basis functions. The discrete implementation of the estimator is facilitated by exploiting certain orthogonality relationships of the transformation matrices such that matrix inversions are not necessary at all. The gravity disturbance vector is obtained in a two-dimensional grid which can be denser than the measurement grid and also at any altitude, including the surface of the earth. Thus, interpolation and downward continuation are performed automatically.

1.7 Overview of Report

This report is organized as follows. Chapter 2 presents the gravity model, whereas Chapter 3 discusses the gravity measurement model. The estimation algorithm is derived in continuous domain in Chapter 4. Discrete implementation of this continuous domain estimator is shown in Chapter 5. Chapter 6 concludes with a brief summary of research performed, highlights of research achievements and suggestions for future research.

2 GRAVITY MODEL

2.1 Introduction & Summary

In this chapter a local gravity model for the survey region is developed. The basis of the model is to represent the unknown mass distribution below the surface of the earth as a two-dimensional white noise layer representing the vertical derivative of the disturbance potential to any pre-specified order. After defining a rectangular survey region, the gravity field in this region for this local white noise layer model is shown to be a linear superposition of a particular solution and a complementary solution. The particular solution involves the solution of Laplace's equation with zero boundary conditions but non-zero sources specified as a two-dimensional white noise layer below the surface of the earth. The complementary solution, on the other hand, involves solution of Laplace's equation with zero sources but non-zero boundary conditions. The contribution from the complementary solution is zero if the boundary conditions are zero. Only the particular solution is addressed since it is assumed that the boundary conditions are zero. The particular solution of the disturbance potential is represented as a series solution, where in the horizontal coordinates the solution involves sine functions due to the zero boundary conditions and in the vertical coordinate it has the form of an exponential function due to the disturbance potential vanishing at infinity. The unknown coefficients of the series expansion represent the random variation, independent of any spatial variation. The condition of uncorrelatedness of the random variables is invoked thereby making the series representation of the disturbance potential a Karhunen-Loève series. An expression for the autocorrelation of the Karhunen-Loève coefficients is obtained from the expression of the white noise layer model representing the vertical derivative of the disturbance potential. Finally, an expression for the covariance of the disturbance potential is obtained which shows that the disturbance potential covariance obtained from this model is both non-stationary and non-isotropic.

2.2 Local Region Spatial Domain

A local region of interest is shown in Figure 2 where x and y coordinates are on the surface of the earth and the z coordinate is vertical above the surface of the earth. The local region of interest is specified by the spatial domain D given as

$$D(x,y) = \{x,y;\ 0 \leq x \leq A,\ 0 \leq y \leq B\} \tag{1}$$

where

A – length of the survey region
B – width of the survey region

The survey measurements are taken at an altitude H above the surface of the earth.

2.3 Local White Noise Layer Model

The gravity field in this local region is completely specified if the following are known:

1) The boundary conditions of this region in terms of the potential values on the boundaries of this region, and

2) The mass distribution density below the surface of the earth within this region.

The model proposed here assumes that the boundary conditions are either known or can be estimated, i.e.

$$T(x, y = 0, z) = f_1(x) \tag{2}$$

$$T(x, y = B, z) = f_2(x) \tag{3}$$

$$T(x = 0, y, z) = g_1(y) \tag{4}$$

$$T(x = A, y, z) = g_2(y) \tag{5}$$

$$T(x, y, z = \pm\infty) = 0 \tag{6}$$

where $T(x, y, z)$ is the anomalous potential or disturbance potential

With respect to the unknown mass distribution below the surface of the earth, the model proposed here is that of a two-dimensional white noise layer representing the kth vertical derivative of the disturbance potential as shown in Figure 2 such that

$$E\left\{\frac{\partial^k T}{\partial z^k}(x_1, y_1, z)\,|_{@z=-D} \times \frac{\partial^k T}{\partial z^k}(x_2, y_2, z)\,|_{@z=-D}\right\} = \sigma_0^2 \delta(x_1 - x_2)\delta(y_1 - y_2) \tag{7}$$

$$0 < x_1, x_2 < A \qquad 0 < y_1, y_2 < B \qquad z = -D$$

where

$\sigma_0{}^2$ - variance of white noise layer
k - order of vertical derivative of T
D - depth of white noise layer

2.4 Linear Superposition Solution

The solution of the disturbance potential with boundary conditions specified by equations (2) through (6) and mass distribution modelled as in equation (7) can be broken up into two parts: the particular solution and the complementary solution (*Boyce* and *DiPrima*, 1969).

The particular solution involves the solution of the three-dimensional Laplace's equation satisfied by the disturbance potential:

$$\left(\frac{\partial^2}{\partial x^2} + \frac{\partial^2}{\partial y^2} + \frac{\partial^2}{\partial z^2}\right) T = 0 \tag{8}$$

with zero boundary conditions

$$T(x = 0, y, z) = 0 \tag{9}$$

$$T(x = A, y, z) = 0 \tag{10}$$

$$T(x, y = 0, z) = 0 \tag{11}$$

$$T(x, y = B, z) = 0 \tag{12}$$

$$T(x, y, z = \pm\infty) = 0 \tag{13}$$

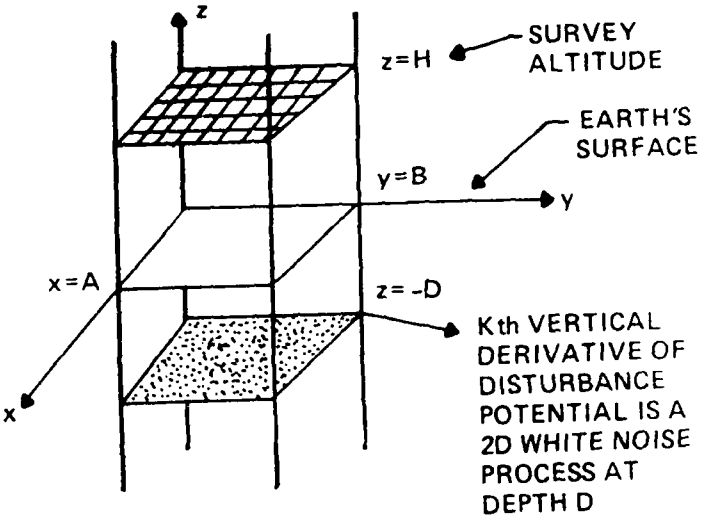

Figure 2: Local White Noise Layer Model

but non-zero sources specified as a two-dimensional white noise layer such as

$$E\left\{\frac{\partial^k T}{\partial z^k}(x_1, y_1, z) \mid_{@z=-D} \times \frac{\partial^k T}{\partial z^k}(x_2, y_2, z) \mid_{@z=-D}\right\} = \sigma_0^2 \delta(x_1 - x_2)\delta(y_1 - y_2) \qquad (14)$$

$$0 < x_1, x_2 < A \qquad 0 < y_1, y_2 < B \qquad z = -D$$

The complementary solution involves the solution of the three-dimensional Laplace's equation satisfied by the disturbance potential:

$$\left(\frac{\partial^2}{\partial x^2} + \frac{\partial^2}{\partial y^2} + \frac{\partial^2}{\partial z^2}\right) T = 0 \qquad (15)$$

with zero sources

$$T = 0 \qquad (16)$$

$$0 < x < A \qquad 0 < y < B \qquad -\infty < z < +\infty$$

but non-zero boundary conditions

$$T(x, y = 0, z) = f_1(x) \qquad (17)$$

$$T(x, y = B, z) = f_2(x) \qquad (18)$$

$$T(x = 0, y, z) = g_1(y) \qquad (19)$$

$$T(x = A, y, z) = g_2(y) \tag{20}$$

$$T(x, y, z = \pm\infty) = 0 \tag{21}$$

In the sequel, only the particular solution is addressed. The complementary solution is zero if the boundary conditions are assumed zero. The rest of this development assumes zero boundary conditions thereby eliminating the need to address the complementary solution any further.

2.5 Series Representation of Potential Function

The basic approach to the solution of the problem is obtained by representing the scalar field $T(x, y, z)$ in a series expansion as follows

$$T(x, y, z) = \sum_{m=1}^{\infty} \sum_{n=1}^{\infty} \alpha_{mn} \phi_{mn}(x, y, z) \tag{22}$$

The above representation of $T(x, y, z)$ implies that

$$T(x, y, z) = \underset{\substack{M \to \infty \\ N \to \infty}}{\text{l.i.m.}} \sum_{m=1}^{M} \sum_{n=1}^{N} \alpha_{mn} \phi_{mn}(x, y, z) \tag{23}$$

where l.i.m. is the limit in the mean square sense such that

$$\underset{\substack{M \to \infty \\ N \to \infty}}{\text{l.i.m.}} \quad E\left\{ \mid T(x, y, z) - \sum_{m=1}^{M} \sum_{n=1}^{N} \alpha_{mn} \phi_{mn}(x, y, z) \mid^2 \right\} = 0 \tag{24}$$

where E is the statistical expectation operator and the functions $\phi_{mn}(x, y, z)$ are complete and square integrable.

Reflecting on equation (22), we observe that by this representation we have separated the random variation from the spatial variation of $T(x, y, z)$. The randomness of $T(x, y, z)$

is included in α_{mn} which is a random variable but independent of any spatial variation. The spatial variation of $T(x, y, z)$, on the other hand, is completely included in $\phi_{mn}(x, y, z)$ which is spatially varying but statistically a deterministic function.

2.6 Particular Solution Spatial Functions

The solution of equation (8) with zero boundary conditions given by equations (9) through (13) is given by using the representation of equation (22) as

$$T(x, y, z) = \frac{2}{\sqrt{AB}} \sum_{m=1}^{\infty} \sum_{n=1}^{\infty} \alpha_{mn} \sin a_m x \sin b_n y e^{-c_{mn}|z+D|} \tag{25}$$

where

$$a_m = \frac{m\pi}{A} \tag{26}$$

$$b_n = \frac{n\pi}{B} \tag{27}$$

$$c_{mn} = (a_m^2 + b_n^2)^{\frac{1}{2}} \tag{28}$$

and α_{mn} are the unknown random coefficients of the series solution.

2.7 Karhunen-Loève Uncorrelatedness of Series Coefficients

The series representation of the disturbance potential given by equation (25) is represented as a Karhunen-Loève Series (*Davenport* and *Root*, 1958) by enforcing the condition of uncorrelatedness of the random variables α_{mn} implying that (*Papoulis*, 1965).

$$E(\alpha_{mn}\alpha_{kl}) = \lambda_{mn}\delta_{mk}\delta_{nl} \tag{29}$$

where λ_{mn} is the correlation of the random variables α_{mn} and the Kronecker delta function is

$$\delta_{ij} = \begin{cases} 1 & i = j \\ 0 & i \neq j \end{cases} \tag{30}$$

2.8 Autocorrelation of Random Variables

An expression for the correlation of the random variables is now obtained by utilizing the condition of uncorrelatedness of the random variables and the two dimensional white noise layer source at depth D.

From equation (25)

$$\frac{\partial^k T}{\partial z^k} = \frac{2(-\operatorname{sgn}(z+D))^k}{\sqrt{AB}} \sum_{m=1}^{\infty}\sum_{n=1}^{\infty} \alpha_{mn} c_{mn}^k \sin(a_m x)\sin(b_n y) e^{-c_{mn}|z+D|} \tag{31}$$

Substituting equation (31) in the left hand side of equation (7) yields

$$E\left\{\frac{\partial^k T}{\partial z^k}(x_1, y_1, z)\,|_{@z=-D} \times \frac{\partial^k T}{\partial z^k}(x_2, y_2, z)\,|_{@z=-D}\right\}$$

$$= \frac{4}{AB} \sum_{m=1}^{\infty}\sum_{n=1}^{\infty}\sum_{k=1}^{\infty}\sum_{l=1}^{\infty} E(\alpha_{mn}\alpha_{kl}) c_{mn}^k c_{kl}^k \sin a_m x_1 \sin b_n y_1 \sin a_k x_2 \sin b_l y_2 \tag{32}$$

Substituting equation (29) in equation (32) reduces the quadruple summation to double summation such that

$$E\left\{\frac{\partial^k T}{\partial z^k}(x_1, y_1, z)\,|_{@z=-D} \times \frac{\partial^k T}{\partial z^k}(x_2, y_2, z)\,|_{@z=-D}\right\}$$

$$= \frac{4}{AB} \sum_{m=1}^{\infty} \sum_{n=1}^{\infty} \lambda_{mn} c_{mn}^{2k} \sin a_m x_1 \sin b_n y_1 \sin a_m x_2 \sin b_n y_2 \tag{33}$$

$$= \frac{4}{AB} \lambda_{mn} c_{mn}^{2k} \sum_{m=1}^{\infty} \sin a_m x_1 \sin a_m x_2 \sum_{n=1}^{\infty} \sin b_n y_1 \sin b_n y_2 \tag{34}$$

where $\lambda_{mn} c_{mn}^{2k}$ is assumed constant. Now, using the series representation of Dirac delta functions

$$\delta(x_1 - x_2) = \frac{2}{A} \sum_{m=1}^{\infty} \sin a_m x_1 \sin a_m x_2 \tag{35}$$

and

$$\delta(y_1 - y_2) = \frac{2}{B} \sum_{n=1}^{\infty} \sin b_n y_1 \sin b_n y_2 \tag{36}$$

in equation (34) yields

$$E \left\{ \frac{\partial^k T}{\partial z^k}(x_1, y_1, z) \mid_{@z=-D} \times \frac{\partial^k T}{\partial z^k}(x_2, y_2, z) \mid_{@z=-D} \right\}$$

$$= \lambda_{mn} c_{mn}^{2k} \delta(x_1 - x_2) \delta(y_1 - y_2) \tag{37}$$

Substituting equation (37) in equation (7) gives

$$\lambda_{mn} c_{mn}^{2k} \delta(x_1 - x_2) \delta(y_1 - y_2) = \sigma_0^2 \delta(x_1 - x_2) \delta(y_1 - y_2) \tag{38}$$

which leads to

$$\lambda_{mn} = \frac{\sigma_0^2}{c_{mn}^{2k}} \tag{39}$$

This is a consequence of assuming a white noise layer. In principle, this assumption could be relaxed to permit any covariance representable in the form given by equation (33). It should be obvious, however, that bounded stationary covariances are ruled out by the zero boundary condition.

2.9 Non-isotropic, Non-stationary Covariance

An expression for the covariance of the disturbance potential is easily obtained by using equations (25) and (29) as follows:

$$R_{TT}(x_1, y_1, z_1; x_2, y_2, z_2)$$

$$= E\{T(x_1, y_1, z_1)T(x_2, y_2, z_2)\}$$

$$= E\left\{\frac{2}{\sqrt{AB}}\sum_{m=1}^{\infty}\sum_{n=1}^{\infty}\alpha_{mn}\sin a_m x_1 \sin b_n y_1 e^{-c_{mn}|z_1+D|}\right.$$

$$\left.\times\frac{2}{\sqrt{AB}}\sum_{k=1}^{\infty}\sum_{l=1}^{\infty}\alpha_{kl}\sin a_k x_2 \sin b_l y_2 e^{-c_{kl}|z_2+D|}\right\}$$

$$= \frac{4}{AB}\sum_{m=1}^{\infty}\sum_{n=1}^{\infty}\sum_{k=1}^{\infty}\sum_{l=1}^{\infty}E(\alpha_{mn}\alpha_{kl})\sin a_m x_1 \sin b_n y_1 \sin a_k x_2 \sin b_l y_2 e^{-c_{mn}|z_1+D|-c_{kl}|z_2+D|}$$

$$= \frac{4}{AB}\sum_{m=1}^{\infty}\sum_{n=1}^{\infty}\lambda_{mn}\sin a_m x_1 \sin b_n y_1 \sin a_m x_2 \sin b_n y_2 e^{-c_{mn}(|z_1+D|+|z_2+D|)} \qquad (40)$$

$$0 < x_1, x_2 < A \qquad 0 < y_1, y_2 < B \qquad -D < z_1, z_2 < +\infty$$

Note that for $z_1, z_2 > -D$ the vertical variation is given as $(z_1 + z_2 + 2D)$ which has the right form as shown by *Moritz* (1980) [page 171].

3 SENSOR MODEL

3.1 Introduction & Summary

In this chapter the mathematical model of the gradiometer sensor is examined. Beginning with the basic definition of the three (3) inline and three (3) crossline gradiometer outputs in terms of the disturbance potential a set of six (6) basis functions are defined in terms of the Karhunen-Loève series expansion of the disturbance potential. These basis functions are shown to be orthogonal within the survey region both individually as well as cumulatively. An expression for the autocorrelation function of the six (6) gradiometer signals taken together is obtained in terms of the basis functions and the autocorrelation of the Karhunen-Loève coefficients. This is then used to derive an integral equation for the gradiometer signal autocorrelation function. The measurements of the inline and crossline gradients are contaminated with additive noise whose autocorrelation function is assumed to be a diagonal matrix.

3.2 Gradiometer Signal Representation

The gradiometer sensor signal $S(x,y,z)$ has six (6) components: three (3) inline signals and three crossline signals. The six (6) signals of the gradiometer are given below

$$S_1(x,y,z) = \frac{1}{2}\left(\frac{\partial^2 T}{\partial x^2} - \frac{\partial^2 T}{\partial y^2}\right) \tag{41}$$

$$S_2(x,y,z) = \frac{1}{2}\left(\frac{\partial^2 T}{\partial y^2} - \frac{\partial^2 T}{\partial z^2}\right) \tag{42}$$

$$S_3(x,y,z) = \frac{1}{2}\left(\frac{\partial^2 T}{\partial z^2} - \frac{\partial^2 T}{\partial x^2}\right) \tag{43}$$

$$S_4(x,y,z) = \frac{\partial^2 T}{\partial x \partial y} \tag{44}$$

$$S_5(x,y,z) = \frac{\partial^2 T}{\partial y \partial z} \tag{45}$$

$$S_6(x,y,z) = \frac{\partial^2 T}{\partial z \partial x} \tag{46}$$

3.3 Definition of basis functions

Taking the appropriate partial derivatives of equation (25) and substituting in equations (41) – (46) gives

$$S_1(x,y,z) = \sum_{m=1}^{\infty}\sum_{n=1}^{\infty} \alpha_{mn} \sin a_m x \sin b_n y \left\{ \frac{-1}{\sqrt{AB}} (a_m^2 - b_n^2) e^{-c_{mn}|z+D|} \right\} \tag{47}$$

$$S_2(x,y,z) = \sum_{m=1}^{\infty}\sum_{n=1}^{\infty} \alpha_{mn} \sin a_m x \sin b_n y \left\{ \frac{-1}{\sqrt{AB}} (c_{mn}^2 + b_n^2) e^{-c_{mn}|z+D|} \right\} \tag{48}$$

$$S_3(x,y,z) = \sum_{m=1}^{\infty}\sum_{n=1}^{\infty} \alpha_{mn} \sin a_m x \sin b_n y \left\{ \frac{1}{\sqrt{AB}} (c_{mn}^2 + a_m^2) e^{-c_{mn}|z+D|} \right\} \tag{49}$$

$$S_4(x,y,z) = \sum_{m=1}^{\infty}\sum_{n=1}^{\infty} \alpha_{mn} \cos a_m x \cos b_n y \left\{ \frac{2}{\sqrt{AB}} a_m b_n e^{-c_{mn}|z+D|} \right\} \tag{50}$$

$$S_5(x,y,z) = \sum_{m=1}^{\infty}\sum_{n=1}^{\infty} \alpha_{mn} \sin a_m x \cos b_n y \left\{ \frac{-2\,\mathrm{sgn}(z+D)}{\sqrt{AB}} b_n c_{mn} e^{-c_{mn}|z+D|} \right\} \tag{51}$$

$$S_6(x,y,z) = \sum_{m=1}^{\infty}\sum_{n=1}^{\infty} \alpha_{mn} \cos a_m x \sin b_n y \left\{ \frac{-2\,\mathrm{sgn}(z+D)}{\sqrt{AB}} a_m c_{mn} e^{-c_{mn}|z+D|} \right\} \tag{52}$$

at $z = H$ these become

$$S_1(x,y) = \sum_{m=1}^{\infty}\sum_{n=1}^{\infty} \alpha_{mn} \sin a_m x \sin b_n y \underbrace{\left\{ \frac{-1}{\sqrt{AB}}(a_m^2 - b_n^2) e^{-c_{mn}|H+D|} \right\}}_{\gamma_{mn1}} \tag{53}$$

$$S_2(x,y) = \sum_{m=1}^{\infty}\sum_{n=1}^{\infty} \alpha_{mn} \sin a_m x \sin b_n y \underbrace{\left\{ \frac{-1}{\sqrt{AB}}(c_{mn}^2 + b_n^2) e^{-c_{mn}|H+D|} \right\}}_{\gamma_{mn2}} \tag{54}$$

$$S_3(x,y) = \sum_{m=1}^{\infty}\sum_{n=1}^{\infty} \alpha_{mn} \sin a_m x \sin b_n y \underbrace{\left\{ \frac{1}{\sqrt{AB}}(c_{mn}^2 + a_m^2) e^{-c_{mn}|H+D|} \right\}}_{\gamma_{mn3}} \tag{55}$$

$$S_4(x,y) = \sum_{m=1}^{\infty}\sum_{n=1}^{\infty} \alpha_{mn} \cos a_m x \cos b_n y \underbrace{\left\{ \frac{2}{\sqrt{AB}} a_m b_n e^{-c_{mn}|H+D|} \right\}}_{\gamma_{mn4}} \tag{56}$$

$$S_5(x,y) = \sum_{m=1}^{\infty}\sum_{n=1}^{\infty} \alpha_{mn} \sin a_m x \cos b_n y \underbrace{\left\{ \frac{-2\,\mathrm{sgn}(H+D)}{\sqrt{AB}} b_n c_{mn} e^{-c_{mn}|H+D|} \right\}}_{\gamma_{mn5}} \tag{57}$$

$$S_6(x,y) = \sum_{m=1}^{\infty}\sum_{n=1}^{\infty} \alpha_{mn} \cos a_m x \sin b_n y \underbrace{\left\{ \frac{-2\,\mathrm{sgn}(H+D)}{\sqrt{AB}} a_m c_{mn} e^{-c_{mn}|H+D|} \right\}}_{\gamma_{mn6}} \tag{58}$$

Representing all six (6) signals of equations (53) through (58) as a vector signal $S(x,y)$ such that

$$S(x,y) = [S_1(x,y) \quad S_2(x,y) \quad S_3(x,y) \quad S_4(x,y) \quad S_5(x,y) \quad S_6(x,y)]^T \tag{59}$$

we obtain

$$S(x,y) = \sum_{m=1}^{\infty}\sum_{n=1}^{\infty}\sum_{i=1}^{6}\alpha_{mn}\psi_{mni}(x,y) \tag{60}$$

$$= \sum_{m=1}^{\infty}\sum_{n=1}^{\infty}\alpha_{mn}\psi_{mn}(x,y) \tag{61}$$

where the individual basis functions ψ_{mni} are defined as

$$\psi_{mn1} = \left[\sin a_m x \sin b_n y \underbrace{\left\{\frac{-1}{\sqrt{AB}}(a_m^2 - b_n^2)e^{-c_{mn}|H+D|}\right\}}_{\gamma_{mn1}} \; 0\;0\;0\;0\;0\right]^T \tag{62}$$

$$\psi_{mn2} = \left[0 \;\sin a_m x \sin b_n y \underbrace{\left\{\frac{-1}{\sqrt{AB}}(c_{mn}^2 + b_n^2)e^{-c_{mn}|H+D|}\right\}}_{\gamma_{mn2}} \; 0\;0\;0\;0\right]^T \tag{63}$$

$$\psi_{mn3} = \left[0\;0 \;\sin a_m x \sin b_n y \underbrace{\left\{\frac{-1}{\sqrt{AB}}(c_{mn}^2 + a_m^2)e^{-c_{mn}|H+D|}\right\}}_{\gamma_{mn3}} \; 0\;0\;0\right]^T \tag{64}$$

$$\psi_{mn4} = \left[0\;0\;0 \;\cos a_m x \cos b_n y \underbrace{\left\{\frac{2}{\sqrt{AB}}a_m b_n e^{-c_{mn}|H+D|}\right\}}_{\gamma_{mn4}} \; 0\;0\right]^T \tag{65}$$

$$\psi_{mn5} = \left[0\ 0\ 0\ 0\ \sin a_m x \cos b_n y \underbrace{\left\{ \frac{-2\,\mathrm{sgn}(H+D)}{\sqrt{A\bar{B}}} b_n c_{mn} e^{-c_{mn}|H+D|} \right\}}_{\gamma_{mn5}} 0 \right] \tag{66}$$

$$\psi_{mn6} = \left[0\ 0\ 0\ 0\ 0\ \cos a_m x \sin b_n y \underbrace{\left\{ \frac{-2\,\mathrm{sgn}(H+D)}{\sqrt{A\bar{B}}} a_m c_{mn} e^{-c_{mn}|H+D|} \right\}}_{\gamma_{mn6}} \right] \tag{67}$$

and the cumulative basis function ψ_{mn} is the sum of the individual basis functions ψ_{mni}

$$\psi_{mn}(x,y) = \sum_{i=1}^{6} \psi_{mni}(x,y) \tag{68}$$

3.4 Orthogonality of Basis Functions

The particular choice of basis functions given by equations (62) - (67) is particularly desirable because they are orthogonal. Orthogonality of these basis functions is examined by evaluating the integral

$$\int_{x=0}^{x=A} \int_{y=0}^{y=B} \psi_{klj}^{T}(x,y) \psi_{mni}(x,y) dx dy$$

for each combination of i,j where $i = 1,2,3,4,5,6$ and $j = 1,2,3,4,5,6$. For example, consider $j = 1$ and $i = 2$, then

$$\int_{x=0}^{x=A} \int_{y=0}^{y=B} [\gamma_{kl1} \sin a_k x \sin b_l y \ \ 0\ \ 0\ \ 0\ \ 0\ \ 0\ \ 0] \begin{bmatrix} 0 \\ \gamma_{mn2} \sin a_m x \sin b_n y \\ 0 \\ 0 \\ 0 \\ 0 \end{bmatrix} dx dy$$

$$= 0 \tag{69}$$

But, when $i = j = 1$, then

$$\int_{x=0}^{x=A} \int_{y=0}^{y=B} \psi_{klj}^{T}(x,y)\psi_{mni}(x,y)dxdy$$

$$= \int_{x=0}^{x=A} \int_{y=0}^{y=B} \psi_{kl1}^{T}(x,y)\psi_{mn1}(x,y)dxdy$$

$$= \int_{x=0}^{x=A} \int_{y=0}^{y=B} [\gamma_{kl1} \sin a_k x \sin b_l y \;\; 0 \;\; 0 \;\; 0 \;\; 0 \;\; 0] \begin{bmatrix} \gamma_{mn1} \sin a_m x \sin b_n y \\ 0 \\ 0 \\ 0 \\ 0 \\ 0 \end{bmatrix} dxdy$$

$$= \int_{x=0}^{x=A} \int_{y=0}^{y=B} \gamma_{kl1}\gamma_{mn1} \sin a_k x \sin b_l y \sin a_m x \sin b_n y dxdy$$

$$= \gamma_{kl1}\gamma_{mn1} \underbrace{\int_{x=0}^{x=A} \sin a_k x \sin a_m x dx}_{\frac{A}{2}\delta_{mk}} \underbrace{\int_{y=0}^{y=B} \sin b_l y \sin b_n y dy}_{\frac{B}{2}\delta_{nl}}$$

$$= \gamma_{kl1}\gamma_{mn1} \frac{AB}{4} \delta_{mk}\delta_{nl} \tag{70}$$

The above results can also be shown to be true for other i, j values using the following identities:

$$\int_{x=0}^{x=A} \sin a_m x \sin a_k x dx = \frac{A}{2}\delta_{mk} \tag{71}$$

$$\int_{y=0}^{y=B} \sin b_n y \sin b_l y dy = \frac{B}{2}\delta_{nl} \tag{72}$$

$$\int_{x=0}^{x=A} \cos a_m x \cos a_k x dx = \frac{A}{2}\delta_{mk} \tag{73}$$

$$\int_{y=0}^{y=B} \cos b_n y \cos b_l y dy = \frac{B}{2}\delta_{nl} \tag{74}$$

where a_m, a_k, b_n, b_l are defined in equations (26) - (27). Thus, individual basis functions defined in equations (62) through (67) are easily seen to be orthogonal satisfying the orthogonality condition given by

$$\int_{x=0}^{x=A}\int_{y=0}^{y=B} \psi_{klj}^T(x,y)\psi_{mni}(x,y)dxdy = \frac{AB}{4}\gamma_{klj}\gamma_{mni}\delta_{mk}\delta_{nl}\delta_{ij} \tag{75}$$

The orthogonality of the cumulative basis functions is examined as shown below.

$$\int_{x=0}^{x=A}\int_{y=0}^{y=B} \psi_{mn}^T\psi_{kl}dxdy$$

$$= \int_{x=0}^{x=A}\int_{y=0}^{y=B} [\gamma_{mn1}\sin a_m x \sin b_n y \quad \gamma_{mn2}\sin a_m x \sin b_n y \quad \gamma_{mn3}\sin a_m x \sin b_n y$$

$$\gamma_{mn4}\cos a_m x \cos b_n y \quad \gamma_{mn5}\sin a_m x \cos b_n y \quad \gamma_{mn6}\cos a_m x \sin b_n y]$$

$$\times \begin{bmatrix} \gamma_{kl1}\sin a_k x \sin b_l y \\ \gamma_{kl2}\sin a_k x \sin b_l y \\ \gamma_{kl3}\sin a_k x \sin b_l y \\ \gamma_{kl4}\cos a_k x \cos b_l y \\ \gamma_{kl5}\sin a_k x \cos b_l y \\ \gamma_{kl1}\cos a_k x \sin b_l y \end{bmatrix} dxdy$$

$$= \gamma_{mn1}\gamma_{kl1} \underbrace{\int_{x=0}^{x=A} \sin a_m x \sin a_k x dx}_{\frac{A}{2}\delta_{mk}} \underbrace{\int_{y=0}^{y=B} \sin b_n y \sin b_l y dy}_{\frac{B}{2}\delta_{nl}}$$

$$+\gamma_{mn2}\gamma_{kl2} \underbrace{\int_{x=0}^{x=A} \sin a_m x \sin a_k x dx}_{\frac{A}{2}\delta_{mk}} \underbrace{\int_{y=0}^{y=B} \sin b_n y \sin b_l y dy}_{\frac{B}{2}\delta_{nl}}$$

$$+\gamma_{mn3}\gamma_{kl3} \underbrace{\int_{x=0}^{x=A} \sin a_m x \sin a_k x dx}_{\frac{A}{2}\delta_{mk}} \underbrace{\int_{y=0}^{y=B} \sin b_n y \sin b_l y dy}_{\frac{B}{2}\delta_{nl}}$$

$$+\gamma_{mn4}\gamma_{kl4} \underbrace{\int_{x=0}^{x=A} \cos a_m x \cos a_k x dx}_{\frac{A}{2}\delta_{mk}} \underbrace{\int_{y=0}^{y=B} \cos b_n y \cos b_l y dy}_{\frac{B}{2}\delta_{nl}}$$

$$+\gamma_{mn5}\gamma_{kl5} \underbrace{\int_{x=0}^{x=A} \sin a_m x \sin a_k x dx}_{\frac{A}{2}\delta_{mk}} \underbrace{\int_{y=0}^{y=B} \cos b_n y \cos b_l y dy}_{\frac{B}{2}\delta_{nl}}$$

$$+\gamma_{mn6}\gamma_{kl6} \underbrace{\int_{x=0}^{x=A} \cos a_m x \cos a_k x dx}_{\frac{A}{2}\delta_{mk}} \underbrace{\int_{y=0}^{y=B} \sin b_n y \sin b_l y dy}_{\frac{B}{2}\delta_{nl}}$$

$$= \gamma_{mn1}\gamma_{kl1}\frac{AB}{4}\delta_{mk}\delta_{nl} + \gamma_{mn2}\gamma_{kl2}\frac{AB}{4}\delta_{mk}\delta_{nl}$$

$$+\gamma_{mn3}\gamma_{kl3}\frac{AB}{4}\delta_{mk}\delta_{nl} + \gamma_{mn4}\gamma_{kl4}\frac{AB}{4}\delta_{mk}\delta_{nl}$$

$$+\gamma_{mn5}\gamma_{kl5}\frac{AB}{4}\delta_{mk}\delta_{nl} + \gamma_{mn6}\gamma_{kl6}\frac{AB}{4}\delta_{mk}\delta_{ni}$$

$$= \frac{AB}{4}\left\{\gamma_{mn1}^2 + \gamma_{mn2}^2 + \gamma_{mn3}^2 + \gamma_{mn4}^2 + \gamma_{mn5}^2 + \gamma_{mn6}^2\right\}\delta_{mk}\delta_{nl}$$

$$= \frac{AB}{4}\sum_{i=1}^{6}\gamma_{mni}\gamma_{kli}\delta_{mk}\delta_{nl} \tag{76}$$

where the γ's are defined in equations (62) - (67). Thus, the cumulative basis functions are also orthogonal satisfying the orthogonality condition given by equation (76).

3.5 Measured Signal Autocorrelation Function

An expression for the autocorrelation function of the gradiometer signals can be obtained using equations (60) and (29) as shown below:

$$R_{SS}(x_1, y_1; x_2, y_2)$$

$$= E\left\{S(x_1, y_1)S^T(x_2, y_2)\right\}$$

$$= E\left\{\left[\sum_{m=1}^{\infty}\sum_{n=1}^{\infty}\sum_{i=1}^{6}\alpha_{mn}\psi_{mni}(x_1, y_1)\right]\left[\sum_{k=1}^{\infty}\sum_{l=1}^{\infty}\sum_{j=1}^{6}\alpha_{kl}\psi_{klj}^T(x_2, y_2)\right]\right.$$

$$= \sum_{m=1}^{\infty}\sum_{n=1}^{\infty}\sum_{i=1}^{6}\sum_{k=1}^{\infty}\sum_{l=1}^{\infty}\sum_{j=1}^{6}\underbrace{E(\alpha_{mn}\alpha_{kl})}_{\lambda_{mn}\delta_{mk}\delta_{nl}}\psi_{mni}(x_1, y_1)\psi_{klj}^T(x_2, y_2)$$

$$= \sum_{m=1}^{\infty} \sum_{n=1}^{\infty} \sum_{i=1}^{6} \sum_{j=1}^{6} \lambda_{mn} \psi_{mni}(x_1, y_1) \psi_{mnj}^T(x_2, y_2) \tag{77}$$

where λ_{mn} was defined in equation (39) and ψ_{mni} is defined in equations (62) - (67).

3.6 Signal Autocorrelation Integral Equation

An integral equation for the measured signal autocorrelation function R_{SS} can be obtained using equations (77) and (75) as shown below:

$$\int_{x_2=0}^{x_2=A} \int_{y_2=0}^{y_2=B} R_{SS}(x_1, y_1; x_2, y_2) \psi_{mni}(x_2, y_2) dx_2 dy_2$$

$$= \int_{x_2=0}^{x_2=A} \int_{y_2=0}^{y_2=B} \sum_{k=1}^{\infty} \sum_{l=1}^{\infty} \sum_{t=1}^{6} \sum_{j=1}^{6} \lambda_{kl} \psi_{klt}(x_1, y_1) \psi_{klj}^T(x_2, y_2) \psi_{mni}(x_2, y_2) dx_2 dy_2$$

$$= \sum_{k=1}^{\infty} \sum_{l=1}^{\infty} \sum_{t=1}^{6} \sum_{j=1}^{6} \lambda_{kl} \psi_{klt}(x_1, y_1) \int_{x_2=0}^{x_2=A} \int_{y_2=0}^{y_2=B} \psi_{klj}^T(x_2, y_2) \psi_{mni}(x_2, y_2) dx_2 dy_2$$

$$= \sum_{k=1}^{\infty} \sum_{l=1}^{\infty} \sum_{t=1}^{6} \sum_{j=1}^{6} \lambda_{kl} \psi_{klt}(x_1, y_1) \frac{AB}{4} \gamma_{klj} \gamma_{mni} \delta_{mk} \delta_{nl} \delta_{ij}$$

$$= \frac{AB}{4} \lambda_{mn} \gamma_{mni}^2 \sum_{t=1}^{6} \psi_{mnt}(x_1, y_1) \tag{78}$$

3.7 Measurement Noise Representation

The measurement $Z(x, y)$ at $z = H$ of the gradiometer signal $S(x, y)$ is contaminated with an additive noise $V(x, y)$ such that

$$Z(x,y) = S(x,y) + V(x,y) \tag{79}$$

The autocorrelation function of the additive noise is assumed to be a diagonal matrix such that

$$R_{VV}(x_1,y_1;x_2,y_2) = \left\{V(x_1,y_1)V^T(x_2,y_2)\right\} \tag{80}$$

$$= \begin{bmatrix} \sigma_1^2 & 0 & 0 & 0 & 0 & 0 \\ 0 & \sigma_2^2 & 0 & 0 & 0 & 0 \\ 0 & 0 & \sigma_3^2 & 0 & 0 & 0 \\ 0 & 0 & 0 & \sigma_4^2 & 0 & 0 \\ 0 & 0 & 0 & 0 & \sigma_5^2 & 0 \\ 0 & 0 & 0 & 0 & 0 & \sigma_6^2 \end{bmatrix} \delta(x_1 - x_2)\delta(y_1 - y_2) \tag{81}$$

The vector signal $S(x,y)$ and measurement noise $V(x,y)$ are assumed to be uncorrelated, i.e.

$$E\left\{S(x_1,y_1)V^T(x_2,y_2)\right\} = \left\{V(x_1,y_1)S^T(x_2,y_2)\right\} = 0 \tag{82}$$

4 ESTIMATION ALGORITHM

4.1 Introduction & Summary

In this chapter an estimation algorithm is developed in the continuous domain. Thus, herein it is assumed that measurements are available in continuous form throughout the survey region. A linear mean square estimation is proposed from which it is shown that estimating the disturbance potential or any functional of the disturbance potential such as the gravity vector or the gravity gradients is equivalent to simply estimating the Karhunen-Leove coefficients. Exploiting the orthogonality principle of linear mean square estimation and the uncorrelatedness of measurement noise and signal leads to a vector integral equation involving the matrix autocorrelation function of the signals to be estimated. This vector integral equation involves the estimator gains which are represented by means of the same orthogonal basis functions with the unknowns being the coefficients of the expansions. An explicit solution of the vector integral equation is then obtained which leads to a closed form solution of the coefficients in the estimator gains. Thus, the estimates of the Karhunen-Loève coefficients are expressed in terms of the coefficients of the estimator gains and measurements integrals of the six (6) gravity gradient measurements. A key result is that the Karhunen-Loève coefficients are estimated utilizing all the gravity gradient measurements simultaneously. Once the Karhunen-Loève coefficients are estimated, the disturbance potential, gravity vector components or gravity gradients can be estimated by utilizing their functional relationships to the Karhunen-Loève coefficients.

4.2 Linear Mean Square Estimation

The desired smoothed estimate $\hat{S}(x,y)$ for the six-dimensional vector signal $S(x,y)$ given by equation (59) is obtained by minimizing the mean square error between the signal $S(x,y)$ and its estimate $\hat{S}(x,y)$ under a performance index $J(x,y)$ defined as

$$J(x,y) = E\left\{|S(x,y) - \hat{S}(x,y)|^2\right\} \tag{83}$$

The optimal estimate $\hat{S}(x,y)$ which minimizes the performance index defined by equation (83) for every point (x,y) in the domain D defined in equation (1) at the measurement altitude $z = H$ is given by (*Papoulis*, 1965)

$$\hat{S}(x,y) = E\left\{S(x,y)|Z(u,v)\right\} \tag{84}$$

$$0 \leq u \leq A \quad 0 \leq v \leq B$$

where the measurements $Z(u,v,H)$ are taken over the entire domain $D(u,v)$ at altitude H. From equation (60) we deduce that

$$\hat{S}(x,y) = \sum_{m=1}^{\infty} \sum_{n=1}^{\infty} \sum_{i=1}^{6} \hat{\alpha}_{mn} \psi_{mni}(x,y) \tag{85}$$

from which we conclude that obtaining $\hat{S}(x,y)$ is equivalent to simply estimating $\hat{\alpha}_{mn}$ from the given measurements $Z(u,v)$. If we assume a linear estimator this can be written as

$$\hat{\alpha}_{mn} = \int_{x=0}^{x=A} \int_{y=0}^{y=B} Z^T(x,y) K_{mn}(x,y) dx dy \tag{86}$$

where $\hat{\alpha}_{mn}$ is a scalar and $Z(x,y)$ and $K_{mn}(x,y)$ are each 6×1 column vectors representing the survey measurements and the estimator gains respectively. In the case of Gaussian statistics, the linear estimator given by equation (86) is equivalent to the general estimator given by equation (84).

4.3 Application of Orthogonality Principle

For linear mean square estimation the orthogonality principle is given by (*Papoulis*, 1965)

$$E\left\{ Z(x_1,y_1) \left[S(x_2,y_2) - \hat{S}(x_2,y_2) \right]^T \right\} = 0 \tag{87}$$

Substituting equations (60) and (85) in the left hand side of equation (87) leads to

$$E\left\{ Z(x_1,y_1) \left[S(x_2,y_2) - \hat{S}(x_2,y_2) \right]^T \right\}$$

$$= E\left\{ Z(x_1,y_1) \left[\sum_{m=1}^{\infty} \sum_{n=1}^{\infty} \sum_{i=1}^{6} \alpha_{mn} \psi_{mni}(x_2,y_2) - \sum_{m=1}^{\infty} \sum_{n=1}^{\infty} \sum_{i=1}^{6} \hat{\alpha}_{mn} \psi_{mni}(x_2,y_2) \right]^T \right\}$$

$$= E\left\{ Z(x_1, y_1) \left[\sum_{m=1}^{\infty} \sum_{n=1}^{\infty} \sum_{i=1}^{6} (\alpha_{mn} - \hat{\alpha}_{mn}) \psi_{mni}(x_2, y_2) \right]^T \right\}$$

$$= E\left\{ Z(x_1, y_1) \sum_{m=1}^{\infty} \sum_{n=1}^{\infty} \sum_{i=1}^{6} (\alpha_{mn} - \hat{\alpha}_{mn}) \psi_{mni}^T(x_2, y_2) \right\}$$

$$= E\left\{ \sum_{m=1}^{\infty} \sum_{n=1}^{\infty} \sum_{i=1}^{6} Z(x_1, y_1)(\alpha_{mn} - \hat{\alpha}_{mn}) \psi_{mni}^T(x_2, y_2) \right\}$$

$$= \sum_{m=1}^{\infty} \sum_{n=1}^{\infty} \sum_{i=1}^{\infty} E\left\{ Z(x_1, y_1)(\alpha_{mn} - \hat{\alpha}_{mn}) \right\} \psi_{mni}^T(x_2, y_2)$$

$$= E\left\{ Z(x_1, y_1)(\alpha_{mn} - \hat{\alpha}_{mn}) \right\}$$

which implies

$$E\left\{ Z(x_1, y_1)\alpha_{mn} \right\} = E\left\{ Z(x_1, y_1)\hat{\alpha}_{mn} \right\} \tag{88}$$

4.4 Uncorrelatedness of Measurement Noise and Coefficients

Substituting the signal representation given by equation (60) into the left hand side of equation (82) leads to

$$E\left\{ V(x_1, y_1) S^T(x_2, y_2) \right\}$$

$$= E\left\{ V(x_1, y_1) \left[\sum_{m=1}^{\infty} \sum_{n=1}^{\infty} \sum_{i=1}^{6} \alpha_{mn} \psi_{mni}(x_2, y_2) \right]^T \right\}$$

$$= E\left\{V(x_1,y_1)\sum_{m=1}^{\infty}\sum_{n=1}^{\infty}\sum_{i=1}^{6}\alpha_{mn}\psi_{mni}^{T}(x_2,y_2)\right\}$$

$$= \sum_{m=1}^{\infty}\sum_{n=1}^{\infty}\sum_{i=1}^{6}E\left\{V(x_1,y_1)\alpha_{mn}\right\}\psi_{mni}^{T}(x_2,y_2)$$

$$= E\left\{V(x_1,y_1)\alpha_{mn}\right\}$$

which implies

$$E\left\{V(x_1,y_1)\alpha_{mn}\right\} = 0 \tag{89}$$

4.5 Integral Equation of Estimator Gains

A vector integral equation involving the matrix autocorrelation functions of the vector signal $S(x,y)$ and the vector estimator gains $K_{mn}(x,y)$ can be obtained as follows:

Using equations (79), (89), (60) , and (29), the left hand side of equation (88) simplifies to

$$E\left\{Z(x_1,y_1)\alpha_{mn}\right\}$$

$$= E\left\{\left[S(x_1,y_1)+V(x_1,y_1)\right]\alpha_{mn}\right\}$$

$$= E\left\{S(x_1,y_1)\alpha_{mn}\right\} + E\left\{V(x_1,y_1)\alpha_{mn}\right\}$$

$$= E\left\{\left[\sum_{k=1}^{\infty}\sum_{l=1}^{\infty}\sum_{j=1}^{6}\alpha_{kl}\psi_{klj}(x_1,y_1)\right]\alpha_{mn}\right\}$$

$$= \sum_{k=1}^{\infty}\sum_{l=1}^{\infty}\sum_{j=1}^{6} E\left\{\alpha_{kl}\alpha_{mn}\right\}\psi_{klj}(x_1,y_1)$$

$$= \sum_{k=1}^{\infty}\sum_{l=1}^{\infty}\sum_{j=1}^{6} \lambda_{kl}\delta_{mk}\delta_{nl}\psi_{klj}(x_1,y_1)$$

$$= \lambda_{mn}\sum_{j=1}^{6}\psi_{mnj}(x_1,y_1) \tag{90}$$

Using equations (86), (79), (82) , and (80), the right hand side of equation (88) simplifies to

$$E\left\{Z(x_1,y_1)\hat{\alpha}_{mn}\right\}$$

$$= E\left\{Z(x_1,y_1)\int_{x_2=0}^{x_2=A}\int_{y_2=0}^{y_2=B} Z^T(x_2,y_2)K_{mn}(x_2,y_2)dx_2dy_2\right\}$$

$$= E\left\{\int_{x_2=0}^{x_2=A}\int_{y_2=0}^{y_2=B} Z(x_1,y_1)Z^T(x_2,y_2)K_{mn}(x_2,y_2)dx_2dy_2\right\}$$

$$= E\left\{\int_{x_2=0}^{x_2=A}\int_{y_2=0}^{y_2=B} \left[S(x_1,y_1)+V(x_1,y_1)\right]\left[S(x_2,y_2)+V(x_2,y_2)\right]^T K_{mn}(x_2,y_2)dx_2dy_2\right\}$$

$$= \int_{x_2=0}^{x_2=A}\int_{y_2=0}^{y_2=B}\left[E\left\{S(x_1,y_1)S^T(x_2,y_2)\right\}+E\left\{S(x_1,y_1)V^T(x_2,y_2)\right\}+E\left\{V(x_1,y_1)S^T(x_2,y_2\right\}\right.$$

$$+ E\left\{V(x_1, y_1)V^T(x_2, y_2)\right\}\Big] K_{mn}(x_2, y_2)dx_2dy_2$$

$$= \int_{x_2=0}^{x_2=A} \int_{y_2=0}^{y_2=B} \{R_{SS}(x_1, y_1; x_2, y_2) + R_{VV}(x_1, y_1; x_2, y_2)\} K_{mn}(x_2, y_2)dx_2dy_2 \quad (91)$$

which is known as the Wiener-Hopf equation. Equating equations (90) and (91) yields

$$\int_{x_2=0}^{x_2=A} \int_{y_2=0}^{y_2=B} \{R_{SS}(x_1, y_1; x_2, y_2) + R_{VV}(x_1, y_1; x_2, y_2)\} K_{mn}(x_2, y_2)dx_2dy_2 = \lambda_{mn} \sum_{j=1}^{6} \psi_{mnj}(x_1, y_1) \quad (92)$$

4.6 Orthogonal Representation of Estimator Gains

The vector estimator gains $K_{mn}(x, y)$ of the linear estimator given by equation (86) can be represented by the orthogonal basis functions given by equations (62) through (67) such that (*Morse* and *Feshbach*, 1953)

$$K_{mn}(x, y) = \sum_{k=1}^{\infty} \sum_{l=1}^{\infty} \sum_{j=1}^{6} \beta_{klj}^{mn} \psi_{klj}(x, y) \quad (93)$$

4.7 Solution of Estimator Gains Integral Equation

The estimator gains $K_{mn}(x, y)$ given by equation (93) have the basis functions $\psi_{klj}(x, y)$ which are known as given in equations (62) through (67) but the β_{klj}^{mn}'s are yet to be determined. An explicit expression for the β_{klj}^{mn}'s is obtained by solving the vector integral equation (92) as follows.

Using equations (93) and (78) in the first half of the left hand side of equation (92) yields

$$\int_{x_2=0}^{x_2=A} \int_{y_2=0}^{y_2=B} R_{SS}(x_1, y_1; x_2, y_2) K_{mn}(x_2, y_2)dx_2dy_2$$

$$= \int_{x_2=0}^{x_2=A} \int_{y_2=0}^{y_2=B} R_{SS}(x_1, y_1; x_2, y_2) \left\{ \sum_{k=1}^{\infty} \sum_{l=1}^{\infty} \sum_{j=1}^{6} \beta_{klj}^{mn} \psi_{klj}(x_2, y_2) \right\} dx_2dy_2$$

$$= \sum_{k=1}^{\infty}\sum_{l=1}^{\infty}\sum_{j=1}^{6}\beta_{klj}^{mn}\int_{x_2=0}^{x_2=A}\int_{y_2=0}^{y_2=B}R_{SS}(x_1,y_1;x_2,y_2)\psi_{klj}(x_2,y_2)dx_2dy_2$$

$$= \sum_{k=1}^{\infty}\sum_{l=1}^{\infty}\sum_{j=1}^{6}\beta_{klj}^{mn}\left\{\frac{AB}{4}\lambda_{kl}\gamma_{klj}^2\sum_{t=1}^{6}\psi_{klt}(x_1,y_1)\right\}$$

$$= \frac{AB}{4}\sum_{k=1}^{\infty}\sum_{l=1}^{\infty}\sum_{j=1}^{6}\sum_{t=1}^{6}\beta_{klj}^{mn}\lambda_{kl}\gamma_{klj}^2\psi_{klt}(x_1,y_1) \tag{94}$$

Using equations (81) and (93) in the second half of the left hand side of equation (92) yields

$$\int_{x_2=0}^{x_2=A}\int_{y_2=0}^{y_2=B}R_{VV}(x_1,y_1;x_2,y_2)K_{mn}(x_2,y_2)dx_2dy_2$$

$$= \int_{x_2=0}^{x_2=A}\int_{y_2=0}^{y_2=B}\begin{bmatrix}\sigma_1^2 & 0 & 0 & 0 & 0 & 0 & 0\\ 0 & \sigma_2^2 & 0 & 0 & 0 & 0 & 0\\ 0 & 0 & \sigma_3^2 & 0 & 0 & 0 & 0\\ 0 & 0 & 0 & \sigma_3^2 & 0 & 0 & 0\\ 0 & 0 & 0 & 0 & \sigma_4^2 & 0 & 0\\ 0 & 0 & 0 & 0 & 0 & \sigma_5^2 & 0\\ 0 & 0 & 0 & 0 & 0 & 0 & \sigma_6^2\end{bmatrix}\delta(x_1-x_2)\delta(y_1-y_2)K_{mn}(x_2,y_2)dx_2dy_2$$

$$= \begin{bmatrix}\sigma_1^2 & 0 & 0 & 0 & 0 & 0 & 0\\ 0 & \sigma_2^2 & 0 & 0 & 0 & 0 & 0\\ 0 & 0 & \sigma_3^2 & 0 & 0 & 0 & 0\\ 0 & 0 & 0 & \sigma_3^2 & 0 & 0 & 0\\ 0 & 0 & 0 & 0 & \sigma_4^2 & 0 & 0\\ 0 & 0 & 0 & 0 & 0 & \sigma_5^2 & 0\\ 0 & 0 & 0 & 0 & 0 & 0 & \sigma_6^2\end{bmatrix}\sum_{k=1}^{\infty}\sum_{l=1}^{\infty}\sum_{j=1}^{6}\beta_{klj}^{mn}\psi_{klj}(x_1,y_1)$$

$$= \sum_{k=1}^{\infty}\sum_{l=1}^{\infty}\sum_{j=1}^{6} \sigma_j^2 \beta_{klj}^{mn} \psi_{klj}(x_1, y_1) \tag{95}$$

The necessity of a diagonal representation for the measurement noise covariance R_{VV} is clear in the derivation of equation (95). Unless, R_{VV} is diagonal, the last step of the derivation of including the variances σ_j^2 within the summation is not possible. This ability to include the variances within the summation sign greatly enhances the analytical tractability of the estimator gains. Substituting equations (94) and (95) in equation (92) leads to

$$\frac{AB}{4} \sum_{k=1}^{\infty}\sum_{l=1}^{\infty}\sum_{j=1}^{6}\sum_{t=1}^{6} \beta_{klj}^{mn} \lambda_{kl} \gamma_{klj}^2 \psi_{klt}(x_1, y_1)$$

$$+ \sum_{k=1}^{\infty}\sum_{l=1}^{\infty}\sum_{j=1}^{6} \sigma_j^2 \beta_{klj}^{mn} \psi_{klj}(x_1, y_1) = \lambda_{mn} \sum_{j=1}^{6} \psi_{mnj}(x_1, y_1) \tag{96}$$

which can be written as

$$\sum_{k=1}^{\infty}\sum_{l=1}^{\infty} \left\{ \sum_{j=1}^{6} \left[\frac{AB}{4} \beta_{klj}^{mn} \lambda_{kl} \gamma_{klj}^2 \sum_{t=1}^{6} \psi_{klt}(x_1, y_1) + \sigma_j^2 \beta_{klj}^{mn} \psi_{klj}(x_1, y_1) \right] \right\} = \lambda_{mn} \sum_{j=1}^{6} \psi_{mnj}(x_1, y_1) \tag{97}$$

Since the right hand side of equation (97) contains no summations on k or l, a unique solution to equation (97) exists if and only if $m = k$ and $n = l$ such that

$$\beta_{klj}^{mn} = \beta_{mnj} \delta_{mk} \delta_{nl} = \begin{cases} \beta_{mnj} & when\ m = k\ and\ n = l \\ 0 & when\ m \neq k\ or\ n \neq l \end{cases} \tag{98}$$

Using equation (98) in equation (93), the estimator gains $K_{mn}(x, y)$ reduce to

$$K_{mn}(x, y) = \sum_{k=1}^{\infty}\sum_{l=1}^{\infty}\sum_{j=1}^{6} \beta_{klj}^{mn} \psi_{klj}(x, y)$$

$$= \sum_{k=1}^{\infty}\sum_{l=1}^{\infty}\sum_{j=1}^{6} \beta_{mnj}\delta_{mk}\delta_{nl}\psi_{klj}(x,y)$$

$$= \sum_{j=1}^{6} \beta_{mnj}\psi_{mnj}(x,y) \tag{99}$$

An expression for the β_{mnj}'s in equation (99) is obtained by substituting equation (98) in equation (97) and solving the resulting equation given by

$$\sum_{j=1}^{6}\left\{\frac{AB}{4}\beta_{mnj}\lambda_{mn}\gamma_{mnj}^2\sum_{t=1}^{6}\psi_{mnt}(x_1,y_1) + \sigma_j^2\beta_{mnj}\psi_{mnj}(x_1,y_1)\right\} = \lambda_{mn}\sum_{j=1}^{6}\psi_{mnj}(x_1,y_1) \tag{100}$$

Multiplying the second term of the LHS by $\sum_{t=1}^{6}\delta_{tj}$, renaming the dummy index j to t on the RHS, and rearranging yields

$$\sum_{t=1}^{6}\left\{\sum_{j=1}^{6}\left\{\frac{AB}{4}\lambda_{mn}\gamma_{mnj}^2 + \delta_{tj}\sigma_j^2\right\}\beta_{mnj} - \lambda_{mn}\right\}\psi_{mnt}(x_1,y_1) = 0 \tag{101}$$

By the linear independence of the $\psi_{mnt}(x_1,y_1)$ equation (101) reduces to

$$\sum_{j=1}^{6}\left\{\frac{AB}{4}\lambda_{mn}\gamma_{mnj}^2 + \delta_{tj}\sigma_j^2\right\}\beta_{mnj} = \lambda_{mn} \tag{102}$$

which can be written in matrix form as

$$\begin{bmatrix} \frac{AB}{4}\lambda_{mn}\gamma_{mn1}^2 + \sigma_1^2 & \frac{AB}{4}\lambda_{mn}\gamma_{mn2}^2 & \cdots & \frac{AB}{4}\lambda_{mn}\gamma_{mn6}^2 \\ \frac{AB}{4}\lambda_{mn}\gamma_{mn1}^2 & \frac{AB}{4}\lambda_{mn}\gamma_{mn2}^2 + \sigma_2^2 & & \frac{AB}{4}\lambda_{mn}\gamma_{mn6}^2 \\ \vdots & & \ddots & \vdots \\ \frac{AB}{4}\lambda_{mn}\gamma_{mn1}^2 & \cdots & & \frac{AB}{4}\lambda_{mn}\gamma_{mn6}^2 + \sigma_6^2 \end{bmatrix}\begin{bmatrix} \beta_{mn1} \\ \beta_{mn2} \\ \vdots \\ \beta_{mn6} \end{bmatrix} = \begin{bmatrix} \lambda_{mn} \\ \lambda_{mn} \\ \vdots \\ \lambda_{mn} \end{bmatrix} \tag{103}$$

By using the method of Gaussian elimination, equation (103) can be solved to yield

$$\beta_{mni} = \frac{\lambda_{mn}}{\sigma_i^2 \left(1 + \frac{AB}{4}\lambda_{mn} \sum_{j=1}^{6} \frac{\gamma_{mnj}^2}{\sigma_j^2}\right)} \tag{104}$$

which can be also written as

$$\beta_{mni} = \frac{\lambda_{mn} \Pi_{j=1, j\neq i}^{6} \sigma_i^2}{\Pi_{j=1}^{6} \sigma_j^2 + \frac{AB}{4}\lambda_{mn} \left(\sum_{j=1}^{6} \gamma_{mnj}^2 \Pi_{k=1, k\neq j}^{6} \sigma_k^2\right)} \tag{105}$$

where the γ_{mnj}'s are given in equations (62) - (67), λ_{mn} is defined in equation (39) and the σ_i's are introduced in equation (81).

4.8 Continuous Domain Measurement Integrals

The estimates of the Karhunen-Loève coefficients α_{mn} are given in terms of the measurements $Z(x,y)$ by equation (86). Using equations (99) and (62) through (67) in equation (86) yields

$$\hat{\alpha}_{mn} = \int_{x=0}^{x=A} \int_{y=0}^{y=B} Z^T(x,y) K_{mn}(x,y) dx dy$$

$$= \int_{x=0}^{x=A} \int_{y=0}^{y=B} Z^T(x,y) \sum_{j=1}^{6} \beta_{mnj} \psi_{mnj}(x,y) dx dy$$

$$= \int_{x=0}^{x=A} \int_{y=0}^{y=B} Z^T(x,y) \{\beta_{mn1}\psi_{mn1}(x,y) + \beta_{mn2}\psi_{mn2}(x,y) + \beta_{mn3}\psi_{mn3}(x,y)$$

$$+\beta_{mn4}\psi_{mn4}(x,y) + \beta_{mn5}\psi_{mn5}(x,y) + \beta_{mn6}\psi_{mn6}(x,y)\} dx dy$$

$$= \int_{x=0}^{x=A} \int_{y=0}^{y=B} Z^T(x,y) \left\{ \beta_{mn1} \begin{bmatrix} \gamma_{mn1} \sin a_m x \sin b_n y \\ 0 \\ 0 \\ 0 \\ 0 \end{bmatrix} + \beta_{mn2} \begin{bmatrix} 0 \\ \gamma_{mn2} \sin a_m x \sin b_n y \\ 0 \\ 0 \\ 0 \end{bmatrix} \right.$$

$$+\beta_{mn3} \begin{bmatrix} 0 \\ 0 \\ \gamma_{mn3} \sin a_m x \sin b_n y \\ 0 \\ 0 \end{bmatrix} + \beta_{mn4} \begin{bmatrix} 0 \\ 0 \\ 0 \\ \gamma_{mn4} \cos a_m x \cos b_n y \\ 0 \end{bmatrix} + \beta_{mn5} \begin{bmatrix} 0 \\ 0 \\ 0 \\ 0 \\ \gamma_{mn5} \sin a_m x \cos b_n y \end{bmatrix}$$

$$\left. + \beta_{mn6} \begin{bmatrix} 0 \\ 0 \\ 0 \\ 0 \\ 0 \\ \gamma_{mn6} \cos a_m x \sin b_n y \end{bmatrix} \right\} dxdy$$

$$= \int_{x=0}^{x=A} \int_{y=0}^{y=B} [Z_1(x,y) \quad Z_2(x,y) \quad Z_3(x,y) \quad Z_4(x,y) \quad Z_5(x,y) \quad Z_6(x,y)]$$

$$\times \begin{bmatrix} \beta_{mn1}\gamma_{mn1} \sin a_m x \sin b_n y \\ \beta_{mn2}\gamma_{mn2} \sin a_m x \sin b_n y \\ \beta_{mn3}\gamma_{mn3} \sin a_m x \sin b_n y \\ \beta_{mn4}\gamma_{mn4} \cos a_m x \cos b_n y \\ \beta_{mn5}\gamma_{mn5} \sin a_m x \cos b_n y \\ \beta_{mn6}\gamma_{mn6} \cos a_m x \sin b_n y \end{bmatrix} dxdy$$

$$= \int_{x=0}^{y=A} \int_{y=0}^{y=B} \{ Z_1(x,y)\beta_{mn1}\gamma_{mn1} \sin a_m x \sin b_n y + Z_2(x,y)\beta_{mn2}\gamma_{mn2} \sin a_m x \sin b_n y$$

$$+Z_3(x,y)\beta_{mn3}\gamma_{mn3}\sin a_m x \sin b_n y + Z_4(x,y)\beta_{mn4}\gamma_{mn4}\cos a_m x \cos b_n y$$

$$+Z_5(x,y)\beta_{mn5}\gamma_{mn5}\sin a_m x \cos b_n y + Z_6(x,y)\beta_{mn6}\gamma_{mn6}\cos a_m x \sin b_n y \;\}$$

$$= \beta_{mn1}\gamma_{mn1}\int_{x=0}^{x=A}\int_{y=0}^{y=B} Z_1(x,y)\sin a_m x \sin b_n y dx dy$$

$$+\beta_{mn2}\gamma_{mn2}\int_{x=0}^{x=A}\int_{y=0}^{y=B} Z_2(x,y)\sin a_m x \sin b_n y dx dy$$

$$+\beta_{mn3}\gamma_{mn3}\int_{x=0}^{x=A}\int_{y=0}^{y=B} Z_3(x,y)\sin a_m x \sin b_n y dx dy$$

$$+\beta_{mn4}\gamma_{mn4}\int_{x=0}^{x=A}\int_{y=0}^{y=B} Z_4(x,y)\cos a_m x \cos b_n y dx dy$$

$$+\beta_{mn5}\gamma_{mn5}\int_{x=0}^{x=A}\int_{y=0}^{y=B} Z_5(x,y)\sin a_m x \cos b_n y dx dy$$

$$+\beta_{mn6}\gamma_{mn6}\int_{x=0}^{x=A}\int_{y=0}^{y=B} Z_6(x,y)\cos a_m x \sin b_n y dx dy$$

$$= \beta_{mn1}\gamma_{mn1}\tilde{Z}_1(m,n) + \beta_{mn2}\gamma_{mn2}\tilde{Z}_2(m,n) + \beta_{mn3}\gamma_{mn3}\tilde{Z}_3(m,n) + \beta_{mn4}\gamma_{mn4}\tilde{Z}_4(m,n)$$

$$+\beta_{mn5}\gamma_{mn5}\tilde{Z}_5(m,n) + \beta_{mn6}\gamma_{mn6}\tilde{Z}_6(m,n) \qquad (106)$$

where

$$\tilde{Z}_1(m,n) = \int_{x=0}^{x=A} \int_{y=0}^{y=B} Z_1(x,y) \sin a_m x \sin b_n y dx dy \tag{107}$$

$$\tilde{Z}_2(m,n) = \int_{x=0}^{x=A} \int_{y=0}^{y=B} Z_2(x,y) \sin a_m x \sin b_n y dx dy \tag{108}$$

$$\tilde{Z}_3(m,n) = \int_{x=0}^{x=A} \int_{y=0}^{y=B} Z_3(x,y) \sin a_m x \sin b_n y dx dy \tag{109}$$

$$\tilde{Z}_4(m,n) = \int_{x=0}^{x=A} \int_{y=0}^{y=B} Z_4(x,y) \cos a_m x \cos b_n y dx dy \tag{110}$$

$$\tilde{Z}_5(m,n) = \int_{x=0}^{x=A} \int_{y=0}^{y=B} Z_5(x,y) \sin a_m x \cos b_n y dx dy \tag{111}$$

$$\tilde{Z}_6(m,n) = \int_{x=0}^{x=A} \int_{y=0}^{y=B} Z_6(x,y) \cos a_m x \sin b_n y dx dy \tag{112}$$

Thus, it is clear that if equations (107) through (112) can be evaluated and substituted in equation (106) along with the β_{mni}'s from equation (105) and the γ_{mni}'s from equations (62) through (67) then the estimates $\hat{\alpha}_{mn}$ of the Karhunen-Loève coefficients can be obtained from equation (106).

4.9 Signal Estimates from Coefficient Estimates

Once the Karhunen-Loève coefficients are estimated, the signal estimates are easily obtained from the basic representation of the disturbance potential $T(x,y,z)$ given by equation (25). Thus, at any spatial point (x,y) in the local region defined by equation (1) and any altitude h, the estimates of the scalar disturbance potential, the three components of the gravity vector and the six elements of the gravity gradients are as given below:

Disturbance Potential Estimate:

$$\widehat{T}(x,y,h) = \sum_{m=1}^{\infty}\sum_{n=1}^{\infty} \hat{\alpha}_{mn} \sin a_m x \sin b_n y \underbrace{\left\{ \frac{2}{\sqrt{AB}} e^{-c_{mn}|h+D|} \right\}}_{\theta_{mn1}} \tag{113}$$

Gravity Vector Estimates:

$$\widehat{\frac{\partial T}{\partial x}}(x,y,h) = \sum_{m=1}^{\infty}\sum_{n=1}^{\infty} \hat{\alpha}_{mn} \cos a_m x \sin b_n y \underbrace{\left\{ \frac{2}{\sqrt{AB}} a_m e^{-c_{mn}|h+D|} \right\}}_{\theta_{mn2}} \tag{114}$$

$$\widehat{\frac{\partial T}{\partial y}}(x,y,h) = \sum_{m=1}^{\infty}\sum_{n=1}^{\infty} \hat{\alpha}_{mn} \sin a_m x \cos b_n y \underbrace{\left\{ \frac{2}{\sqrt{AB}} b_n e^{-c_{mn}|h+D|} \right\}}_{\theta_{mn3}} \tag{115}$$

$$\widehat{\frac{\partial T}{\partial z}}(x,y,h) = \sum_{m=1}^{\infty}\sum_{n=1}^{\infty} \hat{\alpha}_{mn} \sin a_m x \sin b_n y \underbrace{\left\{ \frac{-2\,\mathrm{sgn}(h+D)}{\sqrt{AB}} c_{mn} e^{-c_{mn}|h+D|} \right\}}_{\theta_{mn4}} \tag{116}$$

Gravity Gradient Estimates:

$$\widehat{\frac{\partial^2 T}{\partial x^2}}(x,y,h) = \sum_{m=1}^{\infty}\sum_{n=1}^{\infty} \hat{\alpha}_{mn} \sin a_m x \sin b_n y \underbrace{\left\{ \frac{-2}{\sqrt{AB}} a_m^2 e^{-c_{mn}|h+D|} \right\}}_{\theta_{mn5}} \tag{117}$$

$$\widehat{\frac{\partial^2 T}{\partial y^2}}(x,y,h) = \sum_{m=1}^{\infty}\sum_{n=1}^{\infty} \hat{\alpha}_{mn} \sin a_m x \sin b_n y \underbrace{\left\{ \frac{-2}{\sqrt{AB}} b_n^2 e^{-c_{mn}|h+D|} \right\}}_{\theta_{mn6}} \tag{118}$$

$$\widehat{\frac{\partial^2 T}{\partial z^2}}(x,y,h) = \sum_{m=1}^{\infty}\sum_{n=1}^{\infty} \hat{\alpha}_{mn} \sin a_m x \sin b_n y \underbrace{\left\{ \frac{2}{\sqrt{AB}} c_{mn}^2 e^{-c_{mn}|h+D|} \right\}}_{\theta_{mn7}} \tag{119}$$

$$\widehat{\frac{\partial^2 T}{\partial x \partial y}}(x,y,h) = \sum_{m=1}^{\infty}\sum_{n=1}^{\infty} \hat{\alpha}_{mn} \cos a_m x \cos b_n y \underbrace{\left\{ \frac{2}{\sqrt{AB}} a_m b_n e^{-c_{mn}|h+D|} \right\}}_{\theta_{mn8}} \tag{120}$$

$$\widehat{\frac{\partial^2 T}{\partial y \partial z}}(x,y,h) = \sum_{m=1}^{\infty}\sum_{n=1}^{\infty} \hat{\alpha}_{mn} \sin a_m x \cos b_n y \underbrace{\left\{ \frac{-2\,\mathrm{sgn}(h+D)}{\sqrt{AB}} b_n c_{mn} e^{-c_{mn}|h+D|} \right\}}_{\theta_{mn9}} \tag{121}$$

$$\widehat{\frac{\partial^2 T}{\partial z \partial x}}(x,y,h) = \sum_{m=1}^{\infty}\sum_{n=1}^{\infty} \hat{\alpha}_{mn} \cos a_m x \sin b_n y \underbrace{\left\{ \frac{-2\,\mathrm{sgn}(h+D)}{\sqrt{AB}} a_m c_{mn} e^{-c_{mn}|h+D|} \right\}}_{\theta_{mn10}} \tag{122}$$

5 DISCRETE IMPLEMENTATION

5.1 Introduction & Summary

In this chapter the practical problem of discrete measurements is addressed. The measurements are assumed to be on a regular two-dimensional grid in the survey region. The data samples are assumed to be evenly spaced in each direction although there is no restriction that the sampling interval in either direction need be the same. This is particularly desirable since the measurement samples in airborne gravity gradiometry survey are obtained at a much closer spacing (i.e. 1 Km) on each track even though the spacing between the tracks is further apart (i.e. 5 Km). Since the measurement integrals involve sine and cosine functions a simple application of the Fourier transform formulas result in conversion from integrals to summations. Restricting the spatial frequencies to finite values these double summations are converted to simply left and right transformations involving sine and cosine functions. Assuming that the number of coefficients in the Karhunen-Loève domain is equal to the number of measurements in the spatial domain then an obvious and brute force approach to inverting the measurement integrals is by simply inverting the sine and cosine transformation matrices. The obvious drawback of this approach is the necessity to perform several large matrix inversions. An alternate approach which avoids this drawback altogether is presented. This approach is based on the observation that the sine transform matrices are orthogonal and that the cosine transform matrices also enjoy an orthogonal relationship involving a Toeplitz circulant matrix of alternating ones (1) and zeroes (0). Utilizing these properties the continuous domain measurement integrals are easily discretized for the discrete grid of measurements without any necessity of large scale matrix inversions. It should be pointed out that by this approach the transition from the continuous domain to the discrete domain is exact and not merely a discrete approximation to a continuous algorithm. After this, the estimation of the Karhunen-Loève coefficients becomes a simple matter of point-by-point matrix multiplication (not row-by-column matrix multiplication) and point-by-point matrix summation of the coefficients of the estimator gains, the discretized measurement integrals and observation matrices associated with each of the gradient measurements. Of particular interest, is the fact that all the Karhunen-Loève coefficients are estimated simultaneously using all the discrete two-dimensional grid measurements of all the gradients. Once the Karhunen-Loève coefficient estimates are obtained two-dimensional grid estimates of the disturbance potential, gravity vector components and gravity gradients are easily obtained by point-by-point multiplication of the Karhunen-Loève coefficient estimates with an observation matrix depending on the type of signal to be estimated and subsequently performing appropriate left and right sine and cosine transforms. As before, these transformations involve no matrix inversions. In addition, the two-dimensional grid of signal estimates need not be based on the measurement grid. A finer interpolated or densified grid can be used to obtain the grid of signal estimates. Also this finer grid can be located at any altitude, not necessarily at

the survey altitude by simply specifying the altitude parameters in the observation matrix. Thus downward continuation is performed automatically.

5.2 Definition of Survey Grid

In order to obtain the vector signal estimates for all the spatial points of interest a definition of the two-dimensional grid is necessary. For the present development the two-dimensional grid of data points is defined to be equally spaced in each direction with K data points in the x - direction and L data points in the y - direction. With Δx and Δy the grid spacing in the x and y directions respectively the spatial domain D is given as

$$(K+1)\Delta x = A \qquad 1 \leq k \leq K \tag{123}$$

$$(L+1)\Delta y = B \qquad 1 \leq l \leq L \tag{124}$$

5.3 Application of Fourier Transforms

Applying the theory of Fourier Transforms to the continuous domain measurement integrals given by equations (107) - (112) yields (*Brigham*, 1973)

$$Z_1(x,y) = \frac{4}{AB} \sum_{m=1}^{\infty} \sum_{n=1}^{\infty} \tilde{Z}_1(m,n) \sin a_m x \sin b_n y \tag{125}$$

$$Z_2(x,y) = \frac{4}{AB} \sum_{m=1}^{\infty} \sum_{n=1}^{\infty} \tilde{Z}_2(m,n) \sin a_m x \sin b_n y \tag{126}$$

$$Z_3(x,y) = \frac{4}{AB} \sum_{m=1}^{\infty} \sum_{n=1}^{\infty} \tilde{Z}_3(m,n) \sin a_m x \sin b_n y \tag{127}$$

$$Z_4(x,y) = \frac{4}{AB} \sum_{m=1}^{\infty} \sum_{n=1}^{\infty} \tilde{Z}_4(m,n) \cos a_m x \cos b_n y \tag{128}$$

$$Z_5(x,y) = \frac{4}{AB} \sum_{m=1}^{\infty} \sum_{n=1}^{\infty} \tilde{Z}_5(m,n) \sin a_m x \cos b_n y \tag{129}$$

$$Z_6(x,y) = \frac{4}{AB} \sum_{m=1}^{\infty} \sum_{n=1}^{\infty} \tilde{Z}_6(m,n) \cos a_m x \sin b_n y \tag{130}$$

Limiting the spatial frequencies to

$$1 \leq m \leq M \tag{131}$$

$$1 \leq n \leq N \tag{132}$$

equations (125) through (130) become

$$Z_1(x,y) = \frac{4}{AB} \sum_{m=1}^{M} \sum_{n=1}^{N} \tilde{Z}_1(m,n) \sin a_m x \sin b_n y \tag{133}$$

$$Z_2(x,y) = \frac{4}{AB} \sum_{m=1}^{M} \sum_{n=1}^{N} \tilde{Z}_2(m,n) \sin a_m x \sin b_n y \tag{134}$$

$$Z_3(x,y) = \frac{4}{AB} \sum_{m=1}^{M} \sum_{n=1}^{N} \tilde{Z}_3(m,n) \sin a_m x \sin b_n y \tag{135}$$

$$Z_4(x,y) = \frac{4}{AB} \sum_{m=1}^{M} \sum_{n=1}^{N} \tilde{Z}_4(m,n) \cos a_m x \cos b_n y \tag{136}$$

$$Z_5(x,y) = \frac{4}{AB} \sum_{m=1}^{M} \sum_{n=1}^{N} \tilde{Z}_5(m,n) \sin a_m x \cos b_n y \tag{137}$$

$$Z_6(x,y) = \frac{4}{AB}\sum_{m=1}^{M}\sum_{n=1}^{N}\tilde{Z}_6(m,n)\cos a_m x \sin b_n y \tag{138}$$

Discretizing as per equations (123) and (124) such that

$$x = x_k \qquad 1 \leq k \leq K \tag{139}$$

$$y = y_l \qquad 1 \leq l \leq L \tag{140}$$

and writing in matrix form equations (133) through (138) appear as

$$\underset{K \times L}{[Z_1]} = \frac{4}{AB}\ \underset{K \times M}{[S\Delta X]}\ \underset{M \times N}{\left[\tilde{Z}_1\right]}\ \underset{N \times L}{[S\Delta Y]^T} \tag{141}$$

$$\underset{K \times L}{[Z_2]} = \frac{4}{AB}\ \underset{K \times M}{[S\Delta X]}\ \underset{M \times N}{\left[\tilde{Z}_2\right]}\ \underset{N \times L}{[S\Delta Y]^T} \tag{142}$$

$$\underset{K \times L}{[Z_3]} = \frac{4}{AB}\ \underset{K \times M}{[S\Delta X]}\ \underset{M \times N}{\left[\tilde{Z}_3\right]}\ \underset{N \times L}{[S\Delta Y]^T} \tag{143}$$

$$\underset{K \times L}{[Z_4]} = \frac{4}{AB}\ \underset{K \times M}{[C\Delta X]}\ \underset{M \times N}{\left[\tilde{Z}_4\right]}\ \underset{N \times L}{[C\Delta Y]^T} \tag{144}$$

$$\underset{K \times L}{[Z_5]} = \frac{4}{AB}\ \underset{K \times M}{[S\Delta X]}\ \underset{M \times N}{\left[\tilde{Z}_5\right]}\ \underset{N \times L}{[C\Delta Y]^T} \tag{145}$$

$$\underset{K \times L}{[Z_6]} = \frac{4}{AB} \underset{K \times M}{[C\Delta X]} \underset{M \times N}{\left[\tilde{Z}_6\right]} \underset{N \times L}{[S\Delta Y]^T} \tag{146}$$

where

K, L – Number of measurements in spatial domain x, y plane
M, N – Number of coefficients in Karhunen-Loève domain

and

$$\underset{K \times L}{[Z_1]} = \begin{bmatrix} Z_1(x_1, y_1) & Z_1(x_1, y_2) & \cdots & Z_1(x_1, y_L) \\ Z_1(x_2, y_1) & & & \vdots \\ \vdots & & & \vdots \\ Z_1(x_K, y_1) & \cdots & \cdots & Z_1(x_K, y_L) \end{bmatrix} \tag{147}$$

$$\underset{K \times L}{[Z_2]} = \begin{bmatrix} Z_2(x_1, y_1) & Z_2(x_1, y_2) & \cdots & Z_2(x_1, y_L) \\ Z_2(x_2, y_1) & & & \vdots \\ \vdots & & & \vdots \\ Z_2(x_K, y_1) & \cdots & \cdots & Z_2(x_K, y_L) \end{bmatrix} \tag{148}$$

$$\underset{K \times L}{[Z_3]} = \begin{bmatrix} Z_3(x_1, y_1) & Z_3(x_1, y_2) & \cdots & Z_3(x_1, y_L) \\ Z_3(x_2, y_1) & & & \vdots \\ \vdots & & & \vdots \\ Z_3(x_K, y_1) & \cdots & \cdots & Z_3(x_K, y_L) \end{bmatrix} \tag{149}$$

$$\underset{K \times L}{[Z_4]} = \begin{bmatrix} Z_4(x_1, y_1) & Z_4(x_1, y_2) & \cdots & Z_4(x_1, y_L) \\ Z_4(x_2, y_1) & & & \vdots \\ \vdots & & & \vdots \\ Z_4(x_K, y_1) & \cdots & \cdots & Z_4(x_K, y_L) \end{bmatrix} \tag{150}$$

$$[Z_5]_{\mathrm{K\times L}} = \begin{bmatrix} Z_5(x_1,y_1) & Z_5(x_1,y_2) & \cdots & Z_5(x_1,y_L) \\ Z_5(x_2,y_1) & & & \vdots \\ \vdots & & & \vdots \\ Z_5(x_K,y_1) & \cdots & \cdots & Z_5(x_K,y_L) \end{bmatrix} \tag{151}$$

$$[Z_6]_{\mathrm{K\times L}} = \begin{bmatrix} Z_6(x_1,y_1) & Z_6(x_1,y_2) & \cdots & Z_6(x_1,y_L) \\ Z_6(x_2,y_1) & & & \vdots \\ \vdots & & & \vdots \\ Z_6(x_K,y_1) & \cdots & \cdots & Z_6(x_K,y_L) \end{bmatrix} \tag{152}$$

$$[S\Delta X]_{\mathrm{K\times M}} = \begin{bmatrix} \sin\pi(1\times 1)\frac{\Delta X}{A} & \sin\pi(1\times 2)\frac{\Delta X}{A} & \cdots & \sin\pi(1\times M)\frac{\Delta X}{A} \\ \sin\pi(2\times 1)\frac{\Delta X}{A} & \sin\pi(2\times 2)\frac{\Delta X}{A} & \cdots & \sin\pi(2\times M)\frac{\Delta X}{A} \\ \vdots & & & \\ \sin\pi(K\times 1)\frac{\Delta X}{A} & \sin\pi(K\times 2)\frac{\Delta X}{A} & \cdots & \sin\pi(K\times M)\frac{\Delta X}{A} \end{bmatrix} \tag{153}$$

$$[C\Delta X]_{\mathrm{K\times M}} = \begin{bmatrix} \cos\pi(1\times 1)\frac{\Delta X}{A} & \cos\pi(1\times 2)\frac{\Delta X}{A} & \cdots & \cos\pi(1\times M)\frac{\Delta X}{A} \\ \cos\pi(2\times 1)\frac{\Delta X}{A} & \cos\pi(2\times 2)\frac{\Delta X}{A} & \cdots & \cos\pi(2\times M)\frac{\Delta X}{A} \\ \vdots & & & \\ \cos\pi(K\times 1)\frac{\Delta X}{A} & \cos\pi(K\times 2)\frac{\Delta X}{A} & \cdots & \cos\pi(K\times M)\frac{\Delta X}{A} \end{bmatrix} \tag{154}$$

$$[S\Delta Y]^T_{\mathrm{N\times L}} = \begin{bmatrix} \sin\pi(1\times 1)\frac{\Delta Y}{B} & \sin\pi(1\times 2)\frac{\Delta Y}{B} & \cdots & \sin\pi(1\times L)\frac{\Delta Y}{B} \\ \sin\pi(2\times 1)\frac{\Delta Y}{B} & \sin\pi(2\times 2)\frac{\Delta Y}{B} & \cdots & \sin\pi(2\times L)\frac{\Delta Y}{B} \\ \vdots & & & \\ \sin\pi(N\times 1)\frac{\Delta Y}{B} & \sin\pi(N\times 2)\frac{\Delta Y}{B} & \cdots & \sin\pi(N\times L)\frac{\Delta Y}{B} \end{bmatrix} \tag{155}$$

$$[C\Delta Y]^T_{\mathrm{N\times L}} = \begin{bmatrix} \cos\pi(1\times 1)\frac{\Delta Y}{B} & \cos\pi(1\times 2)\frac{\Delta Y}{B} & \cdots & \cos\pi(1\times L)\frac{\Delta Y}{B} \\ \cos\pi(2\times 1)\frac{\Delta Y}{B} & \cos\pi(2\times 2)\frac{\Delta Y}{B} & \cdots & \cos\pi(2\times L)\frac{\Delta Y}{B} \\ \vdots & & & \\ \cos\pi(N\times 1)\frac{\Delta Y}{B} & \cos\pi(N\times 2)\frac{\Delta Y}{B} & \cdots & \cos\pi(N\times L)\frac{\Delta Y}{B} \end{bmatrix} \tag{156}$$

Thus,

$$[S\Delta X(i,j)] = \sin \pi(i \times j)\frac{\Delta X}{A} \qquad \begin{matrix} 1 \le i \le K \\ 1 \le j \le M \end{matrix} \tag{157}$$

$$[S\Delta Y(i,j)]^T = \sin \pi(i \times j)\frac{\Delta Y}{B} \qquad \begin{matrix} 1 \le i \le N \\ 1 \le j \le L \end{matrix} \tag{158}$$

$$[C\Delta X(i,j)] = \cos \pi(i \times j)\frac{\Delta X}{A} \qquad \begin{matrix} 1 \le i \le K \\ 1 \le j \le M \end{matrix} \tag{159}$$

$$[C\Delta Y(i,j)]^T = \cos \pi(i \times j)\frac{\Delta Y}{B} \qquad \begin{matrix} 1 \le i \le N \\ 1 \le j \le L \end{matrix} \tag{160}$$

5.4 Brute Force Approach Requiring Matrix Inversions

Assuming that the number of coefficients in the Karhunen-Loève domain is equal to the number of measurements in the spatial domain satisfying the conditions

$$M = K \tag{161}$$

$$N = L \tag{162}$$

then an obvious and brute force approach to inverting equations (141) through (146) is by simply inverting the matrices such that

$$\left[\tilde{Z}_1\right] = \frac{AB}{4}\left[S\Delta X\right]^{-1}\left[Z_1\right]\left(\left[S\Delta Y\right]^T\right)^{-1} \tag{163}$$

$$\left[\tilde{Z}_2\right] = \frac{AB}{4}[S\Delta X]^{-1}[Z_2]\left([S\Delta Y]^T\right)^{-1} \tag{164}$$

$$\left[\tilde{Z}_3\right] = \frac{AB}{4}[S\Delta X]^{-1}[Z_3]\left([S\Delta Y]^T\right)^{-1} \tag{165}$$

$$\left[\tilde{Z}_4\right] = \frac{AB}{4}[C\Delta X]^{-1}[Z_4]\left([C\Delta Y]^T\right)^{-1} \tag{166}$$

$$\left[\tilde{Z}_5\right] = \frac{AB}{4}[S\Delta X]^{-1}[Z_5]\left([C\Delta Y]^T\right)^{-1} \tag{167}$$

$$\left[\tilde{Z}_6\right] = \frac{AB}{4}[C\Delta X]^{-1}[Z_6]\left([S\Delta Y]^T\right)^{-1} \tag{168}$$

The obvious drawback of this approach is the necessity to perform several large matrix inversions. In the next section an alternate approach is outlined which avoids this drawback altogether.

5.5 Alternate Approach Avoiding Matrix Inversions

Bose et. al. (1988) have recently shown that the particular matrices under consideration here given by equations (153) through (156) enjoy the following properties outlined below: 1) Sine Transform matrices given by equations (153) and (155) satisfy the condition

$$\underset{K\times K}{[S\Delta X]^T}\,\underset{K\times K}{[S\Delta X]} = \frac{K+1}{2}[I] \tag{169}$$

where [I] is a $K \times K$ identity matrix. The above condition leads to

$$([S\Delta X]^T[S\Delta X])^{-1} = \frac{2}{K+1}[I]$$

or

$$[S\Delta X]^{-1} = \frac{2}{K+1}[S\Delta X]^T \tag{170}$$

2) Cosine transform matrices given by equations (154) and (156) satisfy the condition

$$\underset{K\times K}{[C\Delta X]^T}\underset{K\times K}{[C\Delta X]} = \frac{K+1}{2}[I] - [C] \tag{171}$$

provided K is even and not odd and $[C]$ is a $K \times K$ Toeplitz Circulant matrix of alternating one's (1) and zeroes (0), a 4×4 example of which is

$$[C] = \begin{bmatrix} 1 & 0 & 1 & 0 \\ 0 & 1 & 0 & 1 \\ 1 & 0 & 1 & 0 \\ 0 & 1 & 0 & 1 \end{bmatrix} \tag{172}$$

The properties of Toeplitz Circulant matrices are such that

$$\left(\frac{K+1}{2}[I] - [C]\right)^{-1} = \frac{2}{K+1}([I] + 2[C]) \qquad K - even \tag{173}$$

which leads to

$$([C\Delta X]^T[C\Delta X])^{-1} = \frac{2}{K+1}([I] + 2[C])$$

or

$$[C\Delta X]^{-1} = \frac{2}{K+1}([I] + 2[C])[C\Delta X]^{-1} \tag{174}$$

Using the assumptions given by equations (161) and (162) and the properties given by equations (170) and (174) and the domain definition given by equations (123) and (124)

in equations (141) through (146) yields

$$\underset{K\times L}{[\tilde{Z}_1]} = \frac{AB}{(K+1)(L+1)} \underset{K\times K}{[S\Delta X]^T} \underset{K\times L}{[Z_1]} \underset{L\times L}{[S\Delta Y]} \tag{175}$$

$$\underset{K\times L}{[\tilde{Z}_2]} = \frac{AB}{(K+1)(L+1)} \underset{K\times K}{[S\Delta X]^T} \underset{K\times L}{[Z_2]} \underset{L\times L}{[S\Delta Y]} \tag{176}$$

$$\underset{K\times L}{[\tilde{Z}_3]} = \frac{AB}{(K+1)(L+1)} \underset{K\times K}{[S\Delta X]^T} \underset{K\times L}{[Z_3]} \underset{L\times L}{[S\Delta Y]} \tag{177}$$

$$\underset{K\times L}{[\tilde{Z}_4]} = \frac{AB}{(K+1)(L+1)} \underset{K\times K}{[I+2C]} \underset{K\times K}{[C\Delta X]^T} \underset{K\times L}{[Z_4]} \underset{L\times L}{[C\Delta Y]} \underset{L\times L}{[I+2C]} \tag{178}$$

$$\underset{K\times L}{[\tilde{Z}_5]} = \frac{AB}{(K+1)(L+1)} \underset{K\times K}{[S\Delta X]^T} \underset{K\times L}{[Z_5]} \underset{L\times L}{[C\Delta Y]} \underset{L\times L}{[I+2C]} \tag{179}$$

$$\underset{K\times L}{[\tilde{Z}_6]} = \frac{AB}{(K+1)(L+1)} \underset{K\times K}{[I+2C]} \underset{K\times K}{[C\Delta X]^T} \underset{K\times L}{[Z_6]} \underset{L\times L}{[S\Delta Y]} \tag{180}$$

5.6 Discrete Estimation of Karhunen-Loève Coefficients

Representing $\otimes$ as point-by-point matrix multiplication and not row-by-column matrix multiplication, equation (106), under the assumptions given by equations (161) and (162) can be written in discrete matrix form as

$$\underset{K\times L}{[\hat{\alpha}_{mn}]} = \underset{K\times L}{\beta_{mn1}} \otimes \underset{K\times L}{\tilde{Z}_1(m,n)} \otimes \underset{K\times L}{\gamma_{mn1}} + \underset{K\times L}{\beta_{mn2}} \otimes \underset{K\times L}{\tilde{Z}_2(m,n)} \otimes \underset{K\times L}{\gamma_{mn2}}$$

$$+\underset{K\times L}{\beta_{mn3}}\otimes\underset{K\times L}{\tilde{Z}_3(m,n)}\otimes\underset{K\times L}{\gamma_{mn3}}+\underset{K\times L}{\beta_{mn4}}\otimes\underset{K\times L}{\tilde{Z}_4(m,n)}\otimes\underset{K\times L}{\gamma_{mn4}}$$

$$+\underset{K\times L}{\beta_{mn5}}\otimes\underset{K\times L}{\tilde{Z}_5(m,n)}\otimes\underset{K\times L}{\gamma_{mn5}}+\underset{K\times L}{\beta_{mn6}}\otimes\underset{K\times L}{\tilde{Z}_6(m,n)}\otimes\underset{K\times L}{\gamma_{mn6}} \tag{181}$$

where the β_{mni}'s are given in equation (105), γ_{mni}'s are given in equations (62) through (67) and the $\tilde{Z}_i(m,n)$'s are given in equations (175) through (180).

5.7 Two-dimensional grid estimates of signals

From equations (113) through (122) it is obvious that the signal estimates are available at any altitude h. However, since the estimates of the Karhunen-Loève coefficients are given by equation (181) wherein $\hat{\alpha}_{mn}$ is available in a $K \times L$ matrix form, therefore, in order to obtain the signal estimates the conditions given by equations (161) and (162) are necessary. But the two-dimensional grid of signal estimates need not be based on the measurement grid defined by equations (123) and (124). A finer interpolated grid defined by

$$(P+1)\Sigma X = A \qquad \Sigma X \leq \Delta X \tag{182}$$

$$(Q+1)\Sigma Y = B \qquad \Sigma Y \leq \Delta Y \tag{183}$$

can be used to obtain the grid of signal estimates. Thus, utilizing this grid definition along with necessary conditions given by equations (161) and (162) in equations (113) through (122) yields the following two-dimensional grid of signal estimates.

Disturbance Potential Estimate:

$$\underset{P\times Q}{[\hat{T}]} = \underset{P\times K}{[S\Sigma X]}(\underset{K\times L}{[\hat{\alpha}_{mn}]}\otimes\underset{K\times L}{[\theta_{mnl}]})\underset{L\times Q}{[S\Sigma Y]^T} \tag{184}$$

Gravity Vector Estimates:

$$\underset{P\times Q}{\left[\widehat{\frac{\partial T}{\partial x}}\right]} = \underset{P\times K}{[C\Sigma X]}\underset{K\times L}{([\hat{\alpha}_{mn}]}\otimes\underset{K\times L}{[\theta_{mn2}])}\underset{L\times Q}{[S\Sigma Y]^T} \tag{185}$$

$$\underset{P\times Q}{\left[\widehat{\frac{\partial T}{\partial y}}\right]} = \underset{P\times K}{[S\Sigma X]}\underset{K\times L}{([\hat{\alpha}_{mn}]}\otimes\underset{K\times L}{[\theta_{mn3}])}\underset{L\times Q}{[C\Sigma Y]^T} \tag{186}$$

$$\underset{P\times Q}{\left[\widehat{\frac{\partial T}{\partial z}}\right]} = \underset{P\times K}{[S\Sigma X]}\underset{K\times L}{([\hat{\alpha}_{mn}]}\otimes\underset{K\times L}{[\theta_{mn4}])}\underset{L\times Q}{[S\Sigma Y]^T} \tag{187}$$

Gravity Gradient Estimates:

$$\underset{P\times Q}{\left[\widehat{\frac{\partial^2 T}{\partial x^2}}\right]} = \underset{P\times K}{[S\Sigma X]}\underset{K\times L}{([\hat{\alpha}_{mn}]}\otimes\underset{K\times L}{[\theta_{mn5}])}\underset{L\times Q}{[S\Sigma Y]^T} \tag{188}$$

$$\underset{P\times Q}{\left[\widehat{\frac{\partial^2 T}{\partial y^2}}\right]} = \underset{P\times K}{[S\Sigma X]}\underset{K\times L}{([\hat{\alpha}_{mn}]}\otimes\underset{K\times L}{[\theta_{mn6}])}\underset{L\times Q}{[S\Sigma Y]^T} \tag{189}$$

$$\underset{P\times Q}{\left[\widehat{\frac{\partial^2 T}{\partial z^2}}\right]} = \underset{P\times K}{[S\Sigma X]}\underset{K\times L}{([\hat{\alpha}_{mn}]}\otimes\underset{K\times L}{[\theta_{mn7}])}\underset{L\times Q}{[S\Sigma Y]^T} \tag{190}$$

$$\underset{P\times Q}{\left[\widehat{\frac{\partial^2 T}{\partial x \partial y}}\right]} = \underset{P\times K}{[C\Sigma X]}\underset{K\times L}{([\hat{\alpha}_{mn}]}\otimes\underset{K\times L}{[\theta_{mn8}])}\underset{L\times Q}{[C\Sigma Y]^T} \tag{191}$$

$$\underset{P\times Q}{\left[\widehat{\frac{\partial^2 T}{\partial y \partial z}}\right]} = \underset{P\times K}{[S\Sigma X]}(\underset{K\times L}{[\hat{\alpha}_{mn}]} \otimes \underset{K\times L}{[\theta_{mn9}]})\underset{L\times Q}{[C\Sigma Y]^T} \tag{192}$$

$$\underset{P\times Q}{\left[\widehat{\frac{\partial^2 T}{\partial z \partial x}}\right]} = \underset{P\times K}{[C\Sigma X]}(\underset{K\times L}{[\hat{\alpha}_{mn}]} \otimes \underset{K\times L}{[\theta_{mn10}]})\underset{L\times Q}{[S\Sigma Y]^T} \tag{193}$$

where $\otimes$ has been defined earlier as point-by-point matrix multiplication, θ_{mni}'s are defined in equations (113) through (122) and

$$\underset{P\times K}{[S\Sigma X]} = \begin{bmatrix} \sin\pi(1\times 1)\frac{\Sigma X}{A} & \sin\pi(1\times 2)\frac{\Sigma X}{A} & \cdots & \sin\pi(1\times K)\frac{\Sigma X}{A} \\ \sin\pi(2\times 1)\frac{\Sigma X}{A} & \sin\pi(2\times 2)\frac{\Sigma X}{A} & \cdots & \sin\pi(2\times K)\frac{\Sigma X}{A} \\ \vdots & & & \vdots \\ \sin\pi(P\times 1)\frac{\Sigma X}{A} & \sin\pi(P\times 2)\frac{\Sigma X}{A} & \cdots & \sin\pi(P\times K)\frac{\Sigma X}{A} \end{bmatrix} \tag{194}$$

$$\underset{P\times K}{[C\Sigma X]} = \begin{bmatrix} \cos\pi(1\times 1)\frac{\Sigma X}{A} & \cos\pi(1\times 2)\frac{\Sigma X}{A} & \cdots & \cos\pi(1\times K)\frac{\Sigma X}{A} \\ \cos\pi(2\times 1)\frac{\Sigma X}{A} & \cos\pi(2\times 2)\frac{\Sigma X}{A} & \cdots & \cos\pi(2\times K)\frac{\Sigma X}{A} \\ \vdots & & & \vdots \\ \cos\pi(P\times 1)\frac{\Sigma X}{A} & \cos\pi(P\times 2)\frac{\Sigma X}{A} & \cdots & \cos\pi(P\times K)\frac{\Sigma X}{A} \end{bmatrix} \tag{195}$$

$$\underset{L\times Q}{[S\Sigma Y]^T} = \begin{bmatrix} \sin\pi(1\times 1)\frac{\Sigma Y}{B} & \sin\pi(1\times 2)\frac{\Sigma Y}{B} & \cdots & \sin\pi(1\times Q)\frac{\Sigma Y}{B} \\ \sin\pi(2\times 1)\frac{\Sigma Y}{B} & \sin\pi(2\times 2)\frac{\Sigma Y}{B} & \cdots & \sin\pi(2\times Q)\frac{\Sigma Y}{B} \\ \vdots & & & \vdots \\ \sin\pi(L\times 1)\frac{\Sigma Y}{B} & \sin\pi(L\times 2)\frac{\Sigma Y}{B} & \cdots & \sin\pi(L\times Q)\frac{\Sigma Y}{B} \end{bmatrix} \tag{196}$$

$$\underset{L\times Q}{[C\Sigma Y]^T} = \begin{bmatrix} \cos\pi(1\times 1)\frac{\Sigma Y}{B} & \sin\pi(1\times 2)\frac{\Sigma Y}{B} & \cdots & \cos\pi(1\times Q)\frac{\Sigma Y}{B} \\ \cos\pi(2\times 1)\frac{\Sigma Y}{B} & \sin\pi(2\times 2)\frac{\Sigma Y}{B} & \cdots & \sin\pi(2\times Q)\frac{\Sigma Y}{B} \\ \vdots & & & \vdots \\ \cos\pi(L\times 1)\frac{\Sigma Y}{B} & \sin\pi(L\times 2)\frac{\Sigma Y}{B} & \cdots & \sin\pi(L\times Q)\frac{\Sigma Y}{B} \end{bmatrix} \tag{197}$$

6 CONCLUSIONS

6.1 Summary of Research Performed

A need to devise a methodology to process two-dimensional grids of gravity gradients at survey altitude to yield gravity disturbance vector estimates at the surface of the earth, motivated this research. The measured gravity gradients are the six elements of the gradient tensor. An actual airborne gradiometer survey over an area 300×300 Km consisting of bidirectional flight paths 5 Km apart with along-track sampling intervals of 1 Km will result in approximately 220,000 measurements. The main problem with the determination of the gravity field from airborne gradiometry is the huge amount of gradient data collected during a gradiometry survey. The primary objective of this research effort was to solve the problem of processing all the airborne gravity gradient measurements simultaneously in a computationally efficient manner without neglecting gradiometer measurement noise.

The approach taken here is to exploit the marriage of physical theory of geodesy and random process theory. The gravity signal model used is obtained by solving Laplace's equation with the unknown mass distribution below the surface of the earth modelled as a two-dimensional white noise layer representing the vertical derivative of the disturbance potential to any pre-specified order. This results in a series solution of the disturbance potential wherein the unknown coefficients of the expansion are forced to be uncorrelated by invoking the Karhunen-Loève condition. This resulting disturbance potential covariance obtained from this model is both non-stationary and non-isotropic.

The six (6) gravity gradients being functionals of the disturbance potential were represented in terms of the Karhunen-Loève series expansion of the disturbance potential resulting in six basis functions. These basis functions were shown to be orthogonal. The measurement model was chosen to be these six gravity gradients in the survey region contaminated by additive white noise. The estimation problem was to take all the six gravity gradient measurements in the survey region and obtain estimates of the gravity vector components at the surface. This estimation problem was shown to be equivalent to simply estimating the Karhunen-Loève coefficients from all the gradient measurements.

Under the assumption of gaussianness of noise statistics the optimal estimator was represented by expressing each Karhunen-Loève coefficient as a linear functional of all the measurement data. Each of these linear functionals was specified by an associated weighting function. The form of each weighting function was found by employing the orthogonality principle of linear mean square estimation theory.

The practicality of discrete measurements motivated discretization of the continuous algorithm. Only equally spaced discrete points were considered. Continuous two-dimensional measurement integrals were converted to summations by utilization of special orthogonality properties of sine and cosine transforms discovered during the course of this research. The discrete algorithm turned out to be expressible as a sequence of matrix multiplications without any necessity of matrix inversions whatsoever. It was shown that for evenly spaced

data points the discrete algorithm derived is exact and not merely an approximation to a continuous algorithm.

Once the Karhunen-Loève coefficient estimates were obtained from discrete data, two-dimensional grid estimates of the disturbance potential, gravity vector components and gravity gradients were easily obtained by point-by-point multiplication of the Karhunen-Loève coefficient estimates with an observation matrix depending on the type of signal to be estimated and subsequently performing appropriate left and right sine and cosine transforms. As before, these transformations involve no matrix inversions. In addition, the two-dimensional grid of signal estimates need not be based on the measurement grid. A finer interpolated or densified grid can be used to obtain the grid of signal estimates. Also this finer grid can be located at any altitude, not necessarily at the survey altitude by simply specifying the altitude parameters in the observation matrix. Thus downward continuation is performed automatically.

6.2 Highlights of Research Achievements

A methodology of post-mission data processing for the gravity gradiometer survey system is presented. The highlights of the technique include:

1. The model is derived from the physical theory of geodesy and is not based upon empirical assumptions of correlation functions or power spectral densities.

2. Model can accommodate multiple two-dimensional white noise layers below the surface of the earth.

3. Each layer can model the vertical derivative of the disturbance potential to any order.

4. Non-zero boundary values for the disturbance potential on the exterior of the survey region permitted.

5. The model is such that at any given spatial point the gravity field's correlation with neighboring points is preserved and correlation in any direction is not ignored.

6. The correlation of the gravity field with increasing distance is not ignored.

7. The estimation algorithm does not enforce any unnecessary limitation of causality on the data inasmuch as no one-dimensional scanning is performed.

8. Each coefficient in the series expansion for the gravity field is estimated using all the six inline and crossline gravity gradiometer data simultaneously.

9. The estimation algorithm can handle gradient data given in two-dimensional grids at the same or different altitudes on or above the surface of the earth.

10. Downward continuation of the gravity field from measurements at the survey height above the surface of the earth is automatically done without any loss of accuracy.

11. Interpolation of estimates between grid measurements performed automatically by employing a denser grid for prediction.

12. Different apriori accuracies can be assigned to measurements from different gradiometer inline and crossline measurements.

13. Correlated noise sources can be accommodated to the extent that they can be represented by the basis functions.

14. The estimation algorithm requires no matrix inversions.

15. The discrete algorithm is exact and not merely an approximation to a continuous integral.

16. Measurement data must be in planar gridded form.

6.3 Recommendations for Future Research

Listed below are suggestions for future work to enhance this method of post-mission data processing for the gravity gradiometer survey system:

1. The White Noise Layer (WNL) model used in the algorithm is based on a single layer of white noise below the surface of the earth. Multiple layers can be accommodated and should be investigated to examine its effect on the modeling sensitivity.

2. Other sensors particularly those providing long wavelength information should be incorporated in the estimation algorithm.

3. Measurement error models more elaborate than the present simple white noise model may be worth investigating to better model the measurement errors.

4. Develop implementable algorithms to take care of the non-zero boundary conditions in a manner consistent with survey data.

5. Examine the relationship of this estimator with that of Wiener filtering, Fourier transforms and Least Squares Collocation.

6. Develop algorithms to obtain a theoretical error covariance by using Kronecker matrix products to the discrete algorithm.

7. Use error analysis algorithms to perform combination solution trade-off analysis.

8. Investigate the performance of the algorithm for modeling error both for signal model and for noise models.

9. Investigate optimization of the discrete algorithm from the standpoint of minimizing number of operations as is done in Fast Fourier Transform techniques.

10. Exploit parallel processing techniques to implement the algorithm by means of special purpose microprocessors specifically designed for this algorithm.

11. Investigate applications of the algorithm to fields other than geodesy such as magnetics, atmospheric sciences, topography, image processing, etc.

7 REFERENCES

1. Bellaire, R.G., Statistics of the Geodetic Uncertainties Aloft, *American Geophysical Union Fall Annual Meeting*, San Francisco, December 1971.

2. Bellaire, R.G., A Discus ion of Flat Earth Statistical Models for the Gravity Disturbances and Their Applications, *Proceedings of the International Symposium on Earth Gravity Models and Related Problems*, St. Louis, August 1972.

3. Bellaire, R.G., Correlation Functions on the Upper Half Space, *Bulletin Geodesique*, Vol. 51, No. 2, 1977.

4. Bose, S.C., Mortensen, R.E. and Thobe, G.E., On the Use of Toeplitz Circultant Matrices to Orthogonalize Discrete Cosine Transforms, *IEEE Transactions of Acoustics, Speech and Signal Processing*, accepted for publication, 1988.

5. Boyce, W.E. and DiPrima, R.C., *Elementary Differential Equations and Boundary Value Problems*, John Wiley & Sons, Inc., New York, Second Edition, 1969.

6. Brigham, E. *The Fast Fourier Transform*, Prentice-Hall, Inc., New Jersey, 1973.

7. Brown, R.D., Methods of Processing Gravity Gradiometry Data - Geophysical Applications, *Proceedings of the Second International Symposium on Inertial Technology for Surveying & Geodesy*, Banff, Canada, pp. 569-581, June 1981.

8. Brozena, J.M., A preliminary Analysis of the NRL Airborne Gravimetry System. *Geophysics*, Vol. 49, No. 7, pp. 1060-1069, 1984.

9. Center, J.L. and Peacock, G.S., Techniques for Post-Mission Processing of Gradiometer Survey Data, *Proceedings of the Third International Symposium on Inertial Technology for Surveying and Geodesy*, Volume 2, Banff, Canada, September, 1985.

10. Coons, R.L., Strange, W.E. and Woolard, G.P., Evaluation Study of Airborne Gravimeter Operational Test, University of Wisconsin Geophysical and Polar Research Center Report No. 62-2, 1962.

11. Davenport Jr., , W.B. and Root, W.L., *An Introduction to the Theory of Random Signals and Noise*, McGraw-Hill Book Co., New York, 1958.

12. Eckhardt, D.H., Isomorphic Geodetic and Electrical Networks: An Application to the Analysis of Airborne Gravity Gradiometer Survey Data, *Geophysics*, Volume 51, pp. 2145-2155, November 1986.

13. Forward, R.L., Geodesy with Orbiting Gravity Gradiometers, Research Report No. 442, Hughes Research Laboratories, Malibu, California, 1971.

14. Goldstein, J.D. and White, J.V., A Template Approach to GGSS Data Reduction, *Proceedings of the Thirteenth Moving Base Gravity Gradiometer Conference*, U.S. Air Force Academy, Colorado Springs, Colorado, February 1985.

15. Gumert, W.R. and Cobb, G.E., Helicopter Gravity Measuring System, *Advances in Dynamic Gravimetry*, W.T. Kattner (Editor), pp. 79-83, 1970.

16. Hammer, S.I., Airborne Gravity is Here! *Oil and Gas Journal*, Vol. 80, pp. 113-122, 1982.

17. Hammer, S.I., Airborne Gravity is Here! *Geophysics*, Vol. 48, No. 2, pp. 213-223, 1983.

18. Heller, W.G. and Jordan, S.K. Attenuated White Noise Statistical Gravity model, *Journal of Geophysical Research*, Vol. 84, No. B9, pp. 4680-4688, 1979.

19. Hirvonen, R.A., On the Precision of the Gravimetric Determination of the Geoid, *Transaction of the American Geophysical Union*, Vol. 37, pp. 1-8, 1956.

20. Hirvonen, R.A., Statistical Analysis of Gravity Anomalies, Report No. 19, Dept. of Geodetic Sciences, Ohio State University, Columbus, Ohio, April 1962.

21. Hutcheson, W.J., Frequency Domain Processing of Airborne Gravity Gradiometer Survey System Data for Derivation of Gravity Disturbance Spectrum, *Proceedings of the Thirteenth Moving Base Gravity Gradiometer Conference*, U.S. Air Force Academy, Colorado Springs, Colorado, February 1985.

22. Hutcheson, W.J. and Grierson, A.D., Gravity Gradiometer Post Mission Data Processing, *Proceedings of the Third International Symposium on Inertial Technology for Surveying and Geodesy*, Volume 2, Banff, Canada, September 1985.

23. Jekeli, C., Data processing techniques for airborne gravity gradiometry. *Proceedings of the Beijing International Summer School on Local Gravity Field Approximation*, Beijing, China, August 1984.

24. Jekeli, C. On Optimal Estimation of Gravity from Gravity Gradients at Aircraft Altitude, *Reviews of Geophysics*, Vol. 23, no. 3, pp. 301-311, August 1985.

25. Jekeli, C., Gravity Vector Estimation From a Large and Densely-Spaced Heterogeneous Gradient Data Set Using Closed-Form Kernel Approximations, *Proceedings of the Third International Symposium on Inertial Technology for Surveying and Geodesy*, Banff, Alberta, September 1985.

26. Jordan, S.K., Self-Consistent Statistical Models for the Gravity Anomaly, Vertical Deflections, and Undulation of the Geoid, *Journal of Geophysical Research*, Vol. 77, No. 20, pp. 3660-3670, July 1972.

27. Jordan, S.K., Moving-Base Gravity Gradiometer Surveys and Interpretation. *Geophysics*, Vol. 43, No. 1, pp. 94-101, 1978.

28. Kearsley, W., Estimation of anisotropic characteristics of gravimetric fields, Spring Annual Meeting, American Geophysical Union, Washington, D.C., May 1977.

29. Kearsley, W., Non-stationary estimation in gravity prediction problems, Report No. 256, Department of Geodetic Sciences, Ohio State University, Columbus, Ohio, July 1977.

30. Kasper, Jr., J.F., A Second-Order Markov Gravity Anomaly Model, *Journal of Geophysical Research*, Vol. 76, No. 32, November 1971.

31. Kaula, W.M., Accuracy of Gravimetrically Computed Deflections of the Vertical, *Transactions of the American Geophysical Union*, Vol. 38, No. 3, pp. 297-305, 1957.

32. Kaula, W.M., Statistical and Harmonic Analysis of Gravity, *Journal of Geophysical Research*, Vol. 64, No. 12, pp. 2401-2421, June 1959.

33. LaCoste, L., Ford, J., Bowles, R. and Archer., K., Gravity Measurements in an Airplane using State-of-the-Art Inertial Navigation. *Proceedings of the 47th Annual International Society of Exploration Geophysicists Meeting*, 1977.

34. Lawson, C.L. and Hanson, R.J., *Solving Least Squares Problems*, Prentice-Hall, Inc., Englewood Cliffs NJ, 1974.

35. Levine, S.A. and Gelb, A., Effect of Deflections of the Vertical on the Performance of a Terrestrial Inertial Navigation System, *Journal of Spacecraft and Rockets*, Vol. 6, pp. 978-984, 1969.

36. Meissl, P., Probabilistic Error Analysis of Airborne Gravimetry. Report No. 138, Department of Geodetic Science and Surveying, Ohio State University, Columbus, Ohio, 1970.

37. Metzger, E.H. and Jircitano, A., Application Analysis of Gravity Gradiometers for Mapping of Earth Gravity Anomalies and Derivation of the Density Distribution of the Earth Crust. *Proceedings of the First International Symposium on Inertial Technology for Surveying and Geodesy.* Ottawa, Canada, pp. 334-342, 1977.

38. Metzger, E.H. and Jircitano, A., Application of Bell Rotating Accelerometer Gravity Gradiometers and Gravity Meters to Airborne or Land Vehicle Gravity Surveys. *Proceedings of the Second International Symposium on Inertial Technology for Surveying and Geodesy.* Banff, Canada, pp. 521-535, 1981.

39. Moritz, H., *Advanced Physical Geodesy.* Herbert Winchmann Verlag, Karlsruhe. Abacus Press, Tunbridge Wells, Kent, 1980.

40. Moritz, H., Kinematical Geodesy, Report No. 92, Department of Geodetic Science and Surveying, Ohio State University, Columbus, Ohio, 1967.

41. Moritz, H., Kinematical Geodesy II, Report No. 165, Department of Geodetic Science and Surveying, Ohio State University, Columbus, Ohio, 1971.

42. Morrison, F., Data-dependent least squares collocation for estimating the very short wavelength components of a surface density layer model of the geopotential, Fall Annual Meeting, American Geophysical Union, San Francisco, California, Dec. 1975.

43. Morrison, F., Azimuth dependent statistics for interpolating geodetic data, *Bulletin Geodesique*, Vol. 51, pp. 105-118, 1977.

44. Morse, P.M. and Feshbach, H., *Methods of Theoretical Physics*, McGraw-Hill Book Co., New York, 1953.

45. Nash, Jr., R.A. and Jordan, S.K., Statistical geodesy–an Engineering Perspective, *Proceedings of the IEEE*, Vol. 66, No. 5, pp. 532-550, May 1978.

46. Nettleton, L.L., LaCoste, L. and Harrison, J.C., Tests on an Airborne Gravity Meter, *Geophysics*, Vol. 25 pp. 181-202, 1960.

47. Paik, H.J., Superconducting Tunable-Diaphragm Transducer for Sensitive Acceleration Measurements. *Journal of Applied Physics*, Vol. 47, No. 3, pp. 1168-1178, 1976.

48. Paik, H.J., Superconducting Tensor Gravity Gradiometer. *Proceedings of the Second Inertial Symposium on Inertial Technology for Surveying and Geodesy.* Banff, Canada, pp. 555-568, 1981.

49. Paik, H.J., Review of Superconducting Accelerometer and Gravity Gradiometer Research at the University of Maryland. *Proceedings of the Thirteenth Moving Base Gravity Gradiometer Conference*, Colorado Springs, Colorado, February 1985.

50. Paik, H.J., Mapoles, E.R. and Wong, K.Y., Superconducting Gravity Gradiometers. *Proceedings of the Conference on Future Trends in Superconductive Electronics*, Charlottesville, U.S.A., 1978.

51. Papoulis, *Probability, Random Variables and Stochastic Processes*, McGraw-Hill Book Co., New York, 1965.

52. Peacock, G.S., Post Mission Adjustment of Gravity Gradiometer Data, *Proceedings of the Thirteenth Moving Base Gravity Gradiometer Conference*, Colorado Springs, Colorado, February, 1985.

53. Rufty, A.E., Gradient Integration Procedure for Path Error Reduction, *Proceedings of the Fourteenth Annual Gravity Gradiometry Conference*, Colorado Springs, Colorado February 1986.

54. Rummel, R. and Schwarz, K.P., On the Non-homogeneity of the Global Covariance Function, *Bulletin Geodesique*, Vol. 51, No. 2, pp. 93-103, 1977.

55. Rummel, R., Gravity Parameter Estimation From Large Data Sets Using Stabilized Integral Formulas and a Numerical Integration Based on Discrete Point Data, Report No. 339, Department of Geodetic Science, The Ohio State University, Columbus, Ohio, 1982.

56. Schwarz, K.P., Simulation Study of Airborne Gradiometry, Report No. 253. Department of Geodetic Science and Surveying, Ohio State University, Columbus, Ohio, 1977.

57. Shaw L., Paul, I. and Henrikson, P., Statistical Models for the Vertical Deflection from Gravity Anomaly Models, *Journal of Geophysical Research*, Vol. 74, No. 17, pp. 4259-4265, June 1969.

58. Szabo, B. and Anthony, D., Results of AFGL's Experimental Aerial Gravity measurements. *Bulletin Geodesique*, Vol. 45, pp. 179-202, 1971.

59. Thompson, L.G.D., Airborne Gravity Meter Test. *Journal of Geophysical Research*, Vol. 64, pp. 488-497, 1959.

60. Trageser, M.B., A Gradiometer System for Gravity Anomaly Surveying, Report R-588, The Charles Stark Draper Laboratory, Cambridge, Massachusetts, 1970.

61. Trageser, M.B., Feasibility Model Gravity Gradiometer Test Results, Report P-179, The Charles Stark Draper Laboratory, Cambridge, Massachusetts, 1975.

62. Tscherning, C.G. and Rapp, R.H., Closed Covariance Expressions for Gravity Anomalies, Geoid Undulations, and Deflections of the Vertical Implied by Anomaly Degree Variance Models, Report No. 208, Department of Geodetic Science, Ohio State University, Columbus, Ohio, May 1974.

63. Tscherning, C.G., Covariance Expressions for Second and Lower Order Derivatives of the Anomalous Potential, Report No. 225, Department of Geodetic Science, Ohio State University, Columbus, Ohio, January 1976.

64. Vassiliou, A.A., Comparison of Methods for the Processing of Gravity Gradiometer Data, *Proceedings of the Third International Symposium on Inertial Technology for Surveying and Geodesy*, Volume 2, Banff, Canada, September 1985.

65. Vassiliou, A.A., *Numerical Techniques for Processing Airborne Gradiometer Data*, Ph.D. Thesis, Division of Surveying Engineering, Department of Civil Engineering, The University of Calgary, Calgary, Alberta, May 1986.

66. White, J.V. and Goldstein, J.D., Gravity Gradiometer Survey Data Processing, Report No. AFGL-TR-84-0198 (ADA156165), The Analytic Sciences Corporation, Reading, Massachusetts, 1984.